C−N Bond Formation on Addition of Aryl Carbanions to the Electrophilic Nitrido Ligand in $TpOs(N)Cl_2$

Thomas J. Crevier, Brian K. Bennett, Jake D. Soper, Julie A. Bowman, Ahmad Dehestani, David A. Hrovat, Scott Lovell,† Werner Kaminsky,† and James M. Mayer*

Contribution from the Department of Chemistry, Campus Box 351700, University of Washington, Seattle, Washington 98195-1700

Received August 1, 2000

Abstract: The osmium(VI) nitrido complex $TpOs(N)Cl_2$ (**1**) has been prepared from $K[Os(N)O_3]$ and KTp in aqueous ethanolic HCl. It reacts rapidly with PhMgCl and related reagents with transfer of a phenyl group to the nitrido ligand. This forms Os(IV) metalla-analido complexes, which are readily protonated to give the analido complex $TpOs(NHPh)Cl_2$ (**4**). The nitrido-phenyl derivatives TpOs(N)PhCl and $TpOs(N)Ph_2$ react more slowly with PhMgCl and are not competent intermediates for the reaction of **1** with PhMgCl. Reactions of **1** with alkyl- and arylboranes similarly result in transfer of one organic group to nitrogen, leading to isolable borylamido complexes such as $TpOs[N(Ph)(BPh_2)]Cl_2$ (**11**). This is an unprecedented insertion of a nitrido ligand into a boron−carbon bond. Hydrolysis of **11** gives **4**. Mechanistic studies suggest that both the Grignard and borane reactions proceed by initial weak coordination of Mg or B to the nitrido ligand, followed by migration of the carbanion to nitrogen. The hydrocarbyl group does not go to osmium and then move to nitrogen—there is no change in the atoms bound to the osmium during the reactions. It is suggested that there may be a general preference for nucleophiles to add directly to the metal−ligand multiple bond rather than binding to the metal first and migrating. Ab initio calculations show that the unusual reactivity of **1** results from its accessible LUMO and LUMO + 1, which are the Os≡N π^* orbitals. The bonding in **1** and its reactivity with organoboranes are reminiscent of CO.

Introduction

Metal−ligand multiple bonds are being utilized increasingly both as supporting ligands and as reactive functionalities.[1] Selective oxidations of organic compounds have long been accomplished by metal−oxo complexes, such as osmium tetroxide and permanganate.[2] The use of metal−nitrogen multiple bonds to oxidatively form C−N bonds is more recent, as in the Sharpless osmium oxyamination reaction[3] and the heterogeneous ammoxidation of propylene to acrylonitrile.[4] Metal nitrido compounds ($L_nM{\equiv}N$) are receiving increasing attention because of their potential role in aziridination, nitrogen fixation, and other processes.[1,5,6] New selective C−N bond-forming methodologies are of interest for both fine and commodity chemicals.[7]

The nitrido ligand is an interesting functionality because its reactivity is quite sensitive to the ancillary ligands on the metal center. For example, the nitrido ligand of $[Os(N)R_4]^-$ ($R = CH_2SiMe_3$) is nucleophilic, being alkylated by MeI, while isoelectronic $[Os(N)Cl_4]^-$ is electrophilic, reacting with phosphines at nitrogen.[8] Complexes with electrophilic multiply bonded ligands are good candidates to be oxidants because they can potentially add nucleophiles directly at the ligand; this is now the favored mechanism for OsO_4 oxidations of alkenes.[9]

Reported here are reactions in which carbanions, especially Grignard reagents and organoboranes, add to the electrophilic nitrido ligand in $TpOs(N)Cl_2$ (**1**) (Tp = hydrotris(1-pyrazolyl)-borate).[10] The scope and mechanism of these new C−N bond-forming reactions are described. The data indicate a mechanism of direct addition to the nitrido ligand, without the involvement of an osmium hydrocarbyl intermediate. The importance of the electrophilicity of the nitrido ligand is indicated by experimental

† UW Chemistry departmental crystallographer.

(1) Nugent, W. A.; Mayer, J. M. *Metal−Ligand Multiple Bonds*; John Wiley & Sons: New York, 1988. (b) Parkin, G. In *Progress in Inorganic Chemistry*; Karlin, K. D., ed.; John Wiley & Sons: New York, 1998; Vol. 47, pp 1−167. (c) Dehnicke, K.; Strähle, J. *Angew. Chem., Int. Ed. Engl.* **1992**, *31*, 955−978. (d) Wigley, D. E. *Prog. Inorg. Chem.* **1994**, *42*, 239−482.

(2) Sheldon, R. A.; Kochi, J. K. *Metal-Catalyzed Oxidations of Organic Compounds*; Academic Press: New York, 1981. (b) *Comprehensive Organic Synthesis, Vol. 7, Oxidation*; Trost, B. M., Ed.; Pergamon: New York, 1991. (c) *Organic Syntheses by Oxidation with Metal Compounds*; Mijs, W. J., de Jonge, C. R. H. I., Eds.; Plenum: New York, 1986. (d) Griffith, W. P. *Trans. Met. Chem.* **1990**, *15*, 251−256.

(3) Chong, A. O.; Oshima, K.; Sharpless, *J. Am. Chem. Soc.* **1977**, *99*, 3420.

(4) For a recent overview, see: Olah, G. A.; Molnár, Á. *Hydrocarbon Chemistry*; Wiley: New York, 1995; pp 372−374.

(5) Groves, J. T.; Takahashi, T. *J. Am. Chem. Soc.* **1983**, *105*, 2073−2074. (b) Bottomley, L. A.; Neely, F. L. *J. Am. Chem. Soc.* **1988**, *110*, 6748−6752. du Bois, J.; Tomooka, C. S.; Hong, J.; Carreira, E. M. *Acc. Chem. Res.* **1997**, *30*, 364−372. (c) Cummins, C. C. *Chem. Commun.* **1998**, 1777−1786.

(6) Brown, S. N. *J. Am. Chem. Soc.* **1999**, *121*, 9752−9753. (b) Brown, S. N. *Inorg. Chem.* **2000**, *39*, 378−381.

(7) Recent reviews: (a) Müller, T. E.; Beller, M. *Chem. Rev.* **1998**, *98*, 675−703. (b) Dembech, P.; Seconi, G.; Ricci, A. *Chem. Eur. J.* **2000**, *6*, 1281−1286. (c) Hartwig, J. F. *Angew. Chem., Int. Ed.* **1998**, *37*, 2047−2067. (d) Yang, B. H.; Buchwald, S. L. *J. Organomet. Chem.* **1999**, *576*, 125−146.

(8) Marshman, R. W.; Shapley, P. A. *J. Am. Chem. Soc.* **1990**, *112*, 8369−8378.

(9) DelMonte, A. J.; Haller, J.; Houk, K. N.; Sharpless, K. B.; Singleton, D. A.; Strassner, T.; Thomas, A. A. *J. Am. Chem. Soc.* **1997**, *119*, 9907−9908.

(10) Preliminarly accounts of a portion of this work have appeared. (a) Crevier, T. J.; Mayer, J. M. *J. Am. Chem. Soc.* **1998**, *120*, 5595−5596. (b) Crevier, T. J.; Mayer, J. M. *Angew. Chem., Int. Ed.* **1998**, *37*, 1891.

10.1021/ja0028424 CCC: $20.00
Published on Web 01/23/2001

studies and by density functional calculations. There have been few ab initio studies on transition metal nitrido complexes, and few attempts to explain trends in reactivity using molecular orbital arguments.[11,12]

Results

Synthesis of TpOs(N)Cl$_2$ (1) and Related Compounds. TpOs(N)Cl$_2$ (**1**) is prepared in 35−50% yield by refluxing a mixture of KOs(N)O$_3$,[13] KTp, and aqueous HCl in ethanol for 40 min (eq 1). This very closely follows the procedure for

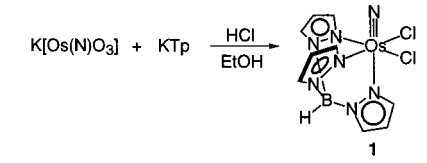

(1)

1

preparation of the isoelectronic rhenium−oxo analogue, TpRe(O)Cl$_2$, from KReO$_4$.[14] Reaction 1 initially turns purple before becoming a brick-red color, from which **1** precipitates as an orange-red solid. The reaction probably proceeds via purple [Os(N)Cl$_5$]$^{2-}$, which is formed immediately upon treating KOs(N)O$_3$ with HCl in ethanol in the absence of KTp.[15] Complex **1** can also be obtained from K$_2$[Os(N)Cl$_5$] or [^{n}Bu$_4$N][Os(N)Cl$_4$] and KTp but in lower yield.[16]

Reaction 1 produces TpOsCl$_3$ as a byproduct, particularly when heating is continued beyond 40 min.[17] Separation of **1** from TpOsCl$_3$ is problematic; our best procedure involves treatment with ferrocene, which removes TpOsCl$_3$ as [Cp$_2$Fe$^+$][TpOsCl$_3^-$].[17] The X-ray crystal structure of **1** purified in this fashion (Tables 1 and 2; Figure 1) shows N/Cl disorder at the nitrido site, refined as 73% N/27% Cl, most likely due to rotational disorder within the crystal.[18] The elongated ellipsoid for the nitrido ligand reflects the difficulty in resolving such disorders, and the Os≡N distance is not accurately determined.[19]

The nitrido-diphenyl derivative, TpOs(N)Ph$_2$ (**3**), is prepared by adding KTp to a solution of [^{n}Bu$_4$N][Os(N)Ph$_2$I$_2$], generated in situ from [^{n}Bu$_4$N][Os(N)Ph$_4$] and aqueous HI (eq 2). This procedure follows Koch and Shapley's preparation of Tp^{Me_2}Os(N)Ph$_2$ from [Os(N)Ph$_2$(py)$_2$]BF$_4$ (Tp^{Me_2} = hydrotris(3,5-dimethyl-1-pyrazolyl)borate).[20] TpOs(N)PhCl (**2**) is formed on treating **3** with HCl (1 M in Et$_2$O) at 70 °C (eq 3). The selective protonolysis of one phenyl group under fairly forcing conditions illustrates the inertness of the Os−Ph bonds.

Table 1. Crystal and Structure Refinement Data for TpOs(N)Cl$_2$ (**1**), TpOs(N)Ph$_2$ (**3**), TpOs(NHPh)Cl$_2$ (**4**), TpOs(NH$_2$Et)Cl$_2$ (**8**), TpOs[N(Ph)BPh$_2$]Cl$_2$ (**11**), TpOs[N(Ph)(PhBOBPh$_2$)]Cl$_2$ (**12**), TpOs(N(C$_6$F$_5$)[B(C$_6$F$_5$)$_2$])Cl$_2$ (**13**), and TpOs[NB(C$_6$F$_5$)$_3$]Ph$_2$ (**17**)[a]

	1	**3**	**4**	**8**[b]	**11**	**12**[c]	**13**[d]	**17**[e]
empirical formula	$C_9H_{10}BCl_2N_7Os$	$C_{21}H_{20}BN_7Os$	$C_{15}H_{16}BCl_2N_7Os$	$C_{14}H_{23}BCl_2N_7OOs$[b]	$C_{27}H_{25}B_2Cl_2N_7Os$	$C_{34}H_{32}B_3Cl_4N_7OO_s$	$C_{30.5}H_{14}B_{2Cl2}F_{15}N_7Os$[c]	$C_{51}H_{32}B_2F_{15}N_7Os$
formula weight	488.15	571.45	566.26	577.30	730.26	919.10	1046.21	1239.66
collection instrument[f]	KappaCCD	KappaCCD	KappaCCD	KappaCCD	CAD4	CAD4	KappaCCD	KappaCCD
crystal system	monoclinic	monoclinic	triclinic	monoclinic	monoclinic	triclinic	monoclinic	triclinic
crystal size (mm)	0.10 × 0.03 × 0.03	0.23 × 0.19 × 0.13	0.16 × 0.11 × 0.06	0.18 × 0.18 × 0.13	0.28 × 0.24 × 0.10	0.38 × 0.34 × 0.30	0.22 × 0.15 × 0.08	0.55 × 0.38 × 0.20
space group	*Cc*	$P2_1/c$	*P*1	$P2_1/m$	*C*2/*c*	*P*1	*C*2/*c*	*P*1
unit cell (Å, deg)								
a	15.1018(12)	15.7489(1)	9.2477(1)	7.6431(2)	21.268(3)	11.578(3)	34.631(2)	11.63800(10)
b	7.6721(7)	17.1382(2)	11.9368(2)	9.9463(3)	9.739(5)	12.343(5)	13.6806(8)	12.7491(2)
c	13.2898(8)	17.2204(1)	18.2652(3)	13.3476(4)	28.269(5)	15.482(5)	16.1004(8)	16.1873(3)
α	90	90	88.336(1)	90	90	91.31(2)	90	94.483(1)
β	108.742(4)	116.175(1)	88.147(1)	91.399(2)	108.88(2)	110.59(2)	116.3750(3)	98.654(1)
γ	90	90	71.989(1)	90	90	115.35(2)	90	101.323(1)
volume (Å^3)	1458.1(2)	4171.28(6)	1916.07(5)	1014.39(5)	5540(3)	1832.0(11)	6833.8(7)	2313.80(6)
Z	4	8	4	2	8	2	8	2
density (g/cm^3, calc)	2.224	1.820	1.963	1.890	1.751	1.666	2.034	1.779
absorption coeff (cm^{-1})	91.10	61.37	69.48	65.67	48.28	38.11	40.08	28.64
temperature (K)	161(2)	161(2)	296(2)	161(2)	183(2)	183(2)	161(2)	161(2)
reflections collected	69944	139 666	51 145	17 170	4258	6391	121 252	96 513
independent reflections	3324	8433	6590	1106	3629	5974	9533	13 918
number of parameters	189	541	469	136	352	451	520	685
final *R*, R_w (%)	5.17, 14.15	2.95, 8.03	4.60, 12.87	2.78, 7.28	3.87, 9.14	5.92, 15.64	7.07, 19.50	4.06, 11.52
goodness of fit	0.984	1.041	0.905	1.098	1.051	1.099	0.976	1.046

[a] The radiation for all structures was Mo Kα (λ = 0.71073 Å). [b] **8** crystallizes as an acetone solvate. [c] **12** crystallizes as a CH_2Cl_2 solvate. [d] **13** crystallizes as a 0.5 toluene solvate. [e] **17** crystallizes as a $2C_6H_6$ solvate. [f] KappaCCD = Nonius KappaCCD; CAD4 = Enraf-Nonius CAD4.

(11) Pandey, K. P.; Sharma, R. B.; Garg, J. *J. Indian Chem. Soc.* **1997**, *74*, 279−283.

(12) Lyne, P. D.; Mingos, M. P. *J. Chem. Soc., Dalton Trans.* **1995**, 1635−1643.

(13) Griffith, W. P. Osmium. In *Comprehensive Coordination Chemistry*; Wilkinson, G., Ed.; Pergamon: New York, 1987; Vol. 4, pp 519−633.

(14) Abrams, M. J.; Davison, A.; Jones, A. G. *Inorg. Chim. Acta* **1984**, *82*, 125−128. (b) Brown, S. N.; Mayer, J. M. *Inorg. Chem.* **1992**, *31*, 4091−4100.

(15) Clifford, A. F.; Kobayahsi, C. S. *Inorg. Synth.* **1960**, *6*, 204−208.

(16) ^{n}Bu$_4$N][Os(N)Cl$_4$] is the starting material for [(trpy)Os(N)Cl$_2$]$^+$ and [(tpm)Os(N)Cl$_2$]$^+$. trpy = 2,2′:6′,2″-terpyridine: (a) Williams, D. S.; Coia, G. M.; Meyer, T. J. *Inorg. Chem.* **1995**, *34*, 586−592. tpm = tris(1-pyrazolyl)methane: (b) Demadis, K. D.; El-Samanody, E.-S.; Meyer, T. J.; White, P. S. *Inorg. Chem.* **1998**, *37*, 383−384. (c) Demadis, K. D.; El-Samanody, E.-S.; Coia, G. M.; Meyer, T. J. *J. Am. Chem. Soc.* **1999**, *121*, 535−544.

(17) Bennett, B. K.; Crevier, T. J.; Mayer, J. M., manuscript in preparation.

(18) The position of the nitrido ligand is independently indicated by the large trans influence, with Os−N$_{pz,trans}$ (2.262(9) Å) almost 0.2 Å longer than Os−N$_{pz,cis}$ (2.082, 2.059(9) Å). (b) For a related example, see: Lincoln, S.; Koch, S. A. *Inorg. Chem.* **1986**, *25*, 1594−1602.

(19) Parkin, G. *Chem. Rev.* **1993**, *93*, 887−911.

(20) Koch, J. L.; Shapley, P. A. *Organometallics* **1997**, *16*, 4071−4076.

Table 2. Selected Bond Lengths (Å) and Angles (Deg) for Os(VI) Nitrido Complexes: Crystallographic Results for **1**, **3**, and **17** and Computational Results (in Italics) for **1** and **18**

	$TpOs(N)Cl_2$ (**1**)	$TpOs(N)Cl_2$ (**1**)	$TpOs(N)Ph_2$ (**3**)[a]	$TpOs(N)Me_2$ (**18**)	$TpOs(NBAr_3)Ph_2$ (**17**)[b]
Os−N(1)	2.262 (9)	*2.103*	2.350 (4)	*2.216*	2.200 (3)
Os−N(3)	2.082(9)	*2.073*	2.150(3)	*2.209*	2.168(3)
Os−N(5)	2.055(8)		2.143(3)		2.119(3)
Os−N(7)	1.70(2)	*1.699*	1.637(4)	*1.676*	1.688(3)
Os−Cl(1)/C(10)	2.295(3)	*2.507*	2.110(4)	*2.154*	2.089(4)
Os−Cl(2)/C(16)	2.317(4)		2.111(4)		2.129(4)
N(7)−Os−N(1)	170.9(10)	*176.4*	174.44(16)	*178.2*	169.56(14)
N(7)−Os−N(3)	92.1(10)	*95.3*	97.53(17)	*99.9*	94.74(13)
N(7)−Os−N(5)	93.8(11)		100.22(16)		106.84(13)
N(7)−Os−Cl(1)/C(10)	100.0(10)	*94.9*	97.15(18)	*94.1*	99.75(14)
N(7)−Os−Cl(2)/C(16)	99.7(10)		95.56(18)		92.90(14)
Cl/C−Os−Cl/C	88.95(15)	*92.3*	89.92(16)	*89.3*	90.71(14)

[a] Data from one of two independent molecules of **3**. [b] Other important bond lengths and angles for **17**: N(7)−B(2), 1.591(5); B(2)−C(22), 1.652(6); B(2)−C(28), 1.626(5); B(2)−C(34), 1.636(6); Os(1)−N(7)−B(2), 167.7(3); N(7)−B(2)−C(22), 107.8(3); N(7)−B(2)−C(28), 101.8(3); N(7)−B(2)−C(34), 111.3(3).

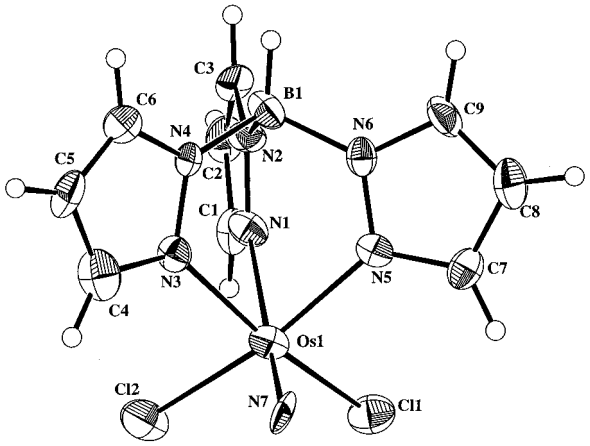

Figure 1. ORTEP diagram of one of the two independent molecules in the crystal of $TpOs(N)Cl_2$ (**1**).

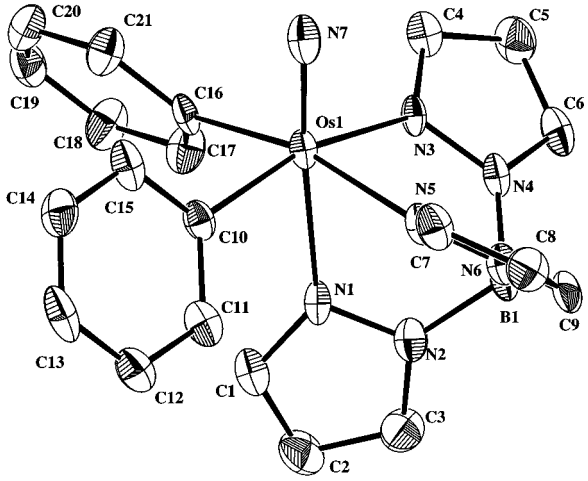

Figure 2. ORTEP diagram of one of the two independent molecules in the crystal of $TpOs(N)Ph_2$ (**3**).

$$[{}^{n}Bu_4N][Os(N)Ph_4] \xrightarrow[\text{acetone}]{\text{1. HI (aq)}\ \text{2. KTp}} \underset{\mathbf{3}}{TpOs(N)Ph_2} \qquad (2)$$

$$\underset{\mathbf{3}}{TpOs(N)Ph_2} \xrightarrow[HCl\ CH_2Cl_2/Et_2O]{\Delta} \underset{\mathbf{2}}{TpOs(N)PhCl} \qquad (3)$$

^1H and ^{13}C NMR spectra of **1**−**3** are consistent with diamagnetic complexes of C_s (**1**, **3**) or C_1 (**2**) symmetry and are similar to the related $TpRe(O)Cl_nPh_{(2-n)}$.[14,21] The IR spectrum of **1** shows peaks typical of octahedral Tp complexes[22] and an Os≡N stretch at 1066 cm^{-1} (Os≡^{15}N, 1036 cm^{-1}; calcd, 1030 cm^{-1}). Meyer et al. report that **1** undergoes an irreversible reduction at −0.98 vs SSCE in MeCN, yielding $[TpCl_2Os^{II}(N_2)\text{-}Os^{III}Cl_2Tp]^-$.[16c] We observe a similar reduction (−1.35 V vs $Cp_2Fe^{+/0}$) and an oxidation wave for **1** at ∼2.05 V.[23] The aryl complexes are harder to reduce (−1.89 V, **2**; −2.04 V, **3**) and easier to oxidize (1.60 V, **2**; 1.36 V, **3**). The X-ray crystal structure of **3** (Tables 1 and 2, Figure 2) is similar to those of **1**, $Tp^{Me_2}Os(N)Ph_2$,[20] and especially $TpRe(O)Ph_2$.[21b] The Os≡N bond lengths, av 1.634 (4) Å in the two independent molecules, are typical of such linkages (1.525−1.703 Å, av 1.629 Å;[24] $Tp^{Me_2}Os(N)Ph_2$, 1.648 (3) Å).

Complexes **1**−**3**, like most of the compounds described here, are air stable and chromatograph well on silica gel. Complex **1** decomposes slowly in CD_2Cl_2 or $CDCl_3$ over roughly a week at 80 °C, yielding some $TpOsCl_3$. **3** is somewhat more stable. The chloride ligands in **1** are quite inert: no exchange is observed with NaI in either acetone or acetonitrile after extended heating, and metathesis with silver salts (e.g., silver acetate) requires heating.[25] Chloride substitution in the related rhenium−oxo and −imido systems $TpRe(E)Cl_2$ is much more facile.[21,26] Complex **1** is unreactive with the electrophiles MeOTf (methyl triflate), $[CF_3C(O)]_2O$, $BF_3{\cdot}Et_2O$, and $[Ph_3C][BF_4]$ at ambient temperatures, with complex reactions occurring over days at 70 °C (as determined by ^1H NMR). This contrasts with the reactivity of many nucleophilic metal nitrido complexes,[1] such as the clean reactions of $CpOs(N)(CH_2SiMe_3)_2$ with MeOTf, $BF_3{\cdot}Et_2O$, and Ag^+.[27] Shapley reports slow alkylation of $Tp^{Me_2}\text{-}Os(N)Ph_2$ by MeOTf,[28] while we find that $TpOs(N)Ph_2$ (**3**) reacts

(21) Brown, S. N.; Mayer, J. M. *J. Am. Chem. Soc.* **1996**, *118*, 12119−12133. (b) Brown, S. N.; Myers, A. W.; Fulton, J. R.; Mayer, J. M. *Organometallics* **1998**, *17*, 3364−3374.

(22) Trofimenko, S. *Chem. Rev.* **1993**, *93*, 943−980 and references therein.

(23) Bennett, B. K.; Crevier, T. J.; DuMez, D. D.; Matano, Y.; McNeil, W. S.; Mayer, J. M. *J. Organomet. Chem.* **1999**, *591*, 96−103.

(24) From a search of the Cambridge Structural Database, January, 1998 release. Allen, F. H.; Kennard, O. *Chem. Des. Autom. News* **1993**, *8*, 31−37.

(25) Dehastani, A.; Bennett, B. K.; Mayer, J. M., work in progress. (b) Crevier, T. J. Ph.D. Thesis, University of Washington, 1998.

(26) McNeil, W. S.; DuMez, D. D.; Matano, Y.; Lovell, S.; Mayer, J. M. *Organometallics* **1999**, *18*, 3715−3727.

(27) Marshman, R. W.; Shusta, J. M.; Wilson, S. R.; Shapley, P. A. *Organometallics* **1991**, *10*, 1671−1676.

(28) Shapley, P. A., personal communication, 1998.

Table 3. Selected Bond Lengths (Å) and Angles (Deg) for Os(IV) Complexes $TpOs(NHPh)Cl_2$ (**4**), $TpOs(NH_2Et)Cl_2$ (**8**), $TpOs[N(Ph)BPh_2]Cl_2$, (**11**), $TpOs[NPh(BPhOBPh_2)]Cl_2$ (**12**), and $TpOs(N(C_6F_5)[B(C_6F_5)_2])Cl_2$ (**13**)[a]

	4[b]	**8**	**11**[c]	**12**[d]	**13**[d]
$Os-N_{amide}$	1.919(6)	2.129(8)[e]	1.880(10)	1.939(7)	2.057(7)
$Os-N_{trans}$[a]	2.097(5)	2.056(8)	2.103(9)	2.074(7)	2.075(7)
$Os-N_{cis1}$[a]	2.052(6)	2.051(5)	2.031(9)	2.038(7)	2.026(8)
$Os-N_{cis2}$[a]	2.039(6)		2.065(10)	2.038(7)	2.036(8)
Os−Cl(1)	2.363(2)	2.3707(19)	2.403(3)	2.363(2)	2.323(3)
Os−Cl(2)	2.384(2)		2.355(3)	2.372(2)	2.308(2)
$N_{amide}-C(10)$	1.384(9)	1.501(13)[e,f]	1.405(15)	1.396(11)	1.461(11)
$N_{amide}-B(2)$			1.602(16)	1.507(12)	1.408(14)
B(2)−C(16)			1.607(19)	1.570(15)	1.583(15)
B(2)−C(22)/O			1.60(2)	1.344(13)	1.632(18)
B(2)−Cl(1)			2.069(15)		
B(3)−O				1.406(13)	1.406(13)
$N_{amide}-Os-N_{trans}$	178.9(2)	179.9(2)[e]	172.5(4)	178.9(3)	173.7(3)
$N_{amide}-Os-N_{cis1}$	93.7(3)	93.4(2)[e]	97.4(4)	96.8(3)	91.0(3)
$N_{amide}-Os-N_{cis2}$	94.6(2)		93.6(4)	93.5(3)	94.0(3)
N_{amide}−Os−Cl(1)	90.94(18)	88.06(15)[e]	75.7(3)	89.9(2)	93.0(2)
N_{amide}−Os−Cl(2)	89.88(19)		100.3(3)	93.1(2)	94.8(2)
Cl(1)−Os−Cl(2)	90.69(9)	91.21(9)	89.24(12)	90.78(9)	89.31(9)
$Os-N_{amide}-C(10)$	133.8(5)	122.0(6)[e,f]	127.9(8)	127.6(6)	115.7(5)
$Os-N_{amide}-B(2)$			112.0(7)	115.6(5)	130.6(7)
$C(10)-N_{amide}-B(2)$			119.3(10)	116.7(7)	113.7(8)

[a] N_{trans} and N_{cis} refer to the relationship to N_{amide}. [b] Data from one of two independent molecules. [c] Other angles for **11**: N(7)−B(2)−C(16), 114.9(11); N(7)−B(2)−C(22), 115.3(10); N(7)−B(2)−Cl(1), 92.0(7); C(16)−B(2)−C(22), 116.3(11); C(16)−B(2)−Cl(1), 105.8(9); C(22)−B(2)−Cl(1), 108.9(9); Os−Cl(1)−B(2), 80.2(4). [d] Other bond lengths and angles for **12**: B(3)−C(22), 1.578(14); B(3)−C(28), 1.581(14); O−B(2)−N(7), 121.7(9); O−B(2)−C(16), 118.7(8); N(7)−B(2)-C(16), 119.4(8); B(2)−O−B(3), 138.6(8); O−B(3)−C(28), 116.2(8); O−B(3)−C(22), 116.4(8); C(22)−B(3)−C(28), 121.3(8). [e] Distance or angle involving N_{amine}. [f] Distance or angle involving C(5).

with excess MeOTf in $CDCl_3$ only upon heating at 70 °C for a day, leading to decomposition. Changing chloride for phenyl and changing Tp to Tp^{Me_2} both affect the reactivity of the nitrido ligands, as well as the redox potentials of the complexes.[23]

Reactions with Grignard and Related Reagents. Addition of 1 equiv of PhMgCl to an ether solution of $TpOs(N)Cl_2$ (**1**) at −78 °C gives a dark orange solution, which turns bright red on exposure to air. Aerobic workup and chromatography on silica gel give the red-purple osmium(IV) analido complex $TpOs(NHPh)Cl_2$ (**4**) (eq 4). Similar results are obtained in THF

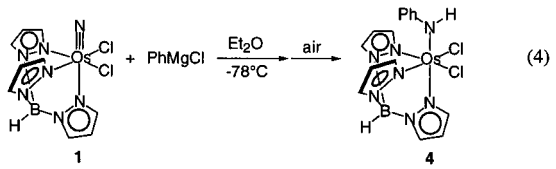

(4)

or toluene, and using PhMgBr, PhLi, or "Ph_3ZnLi" (3PhLi + $ZnCl_2$) as the arylating agents. Phenyl cuprates, however, gave low and irreproducible yields of the Cl metathesis products **2** and/or **3**.

Compound **4** has a mildly paramagnetically shifted ^1H NMR spectrum with sharp lines, as is typical for d^4 octahedral Os and Re complexes.[29] Mass spectrometry shows a strong parent ion cluster with the characteristic isotope pattern, along with clusters for M^+-Cl and M^+-NHPh. The IR spectrum of **4** shows a somewhat broad peak at 3519 cm^{-1} due to the amido proton. Workup with D_2O instead of air (see below) gives **4**-d_1, in which the characteristic N*H* resonance at δ 5.87 is absent in the ^1H NMR. The X-ray structure of **4** (Tables 1 and 3, Figure 3) shows two independent molecules with nearly identical bond lengths and angles, and no evidence of intermolecular interactions. The coordination geometry about osmium is roughly octahedral, with the phenyl group of the analido ligand interleaved between two pyrazoles.

(29) For example: Randall. E. W.; Shaw, D. *J. Chem. Soc. A* **1969**, 2867−2872.

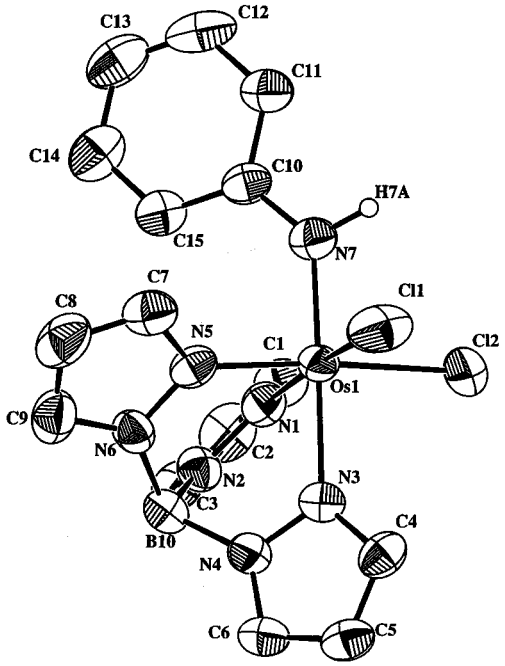

Figure 3. ORTEP diagram of one of the two independent molecules in the crystal of $TpOs(NHPh)Cl_2$ (**4**).

Addition of tolylmagnesium bromide to **1** and workup gives the tolyl derivative $TpOs(NHTol)Cl_2$ (**5**). Interestingly, **5** is also formed on reaction of **1** with *p*-toluidine (H_2NTol) over 3 days at 70 °C.[25b] Reaction of **1** with 2 or 3 equiv of phenyl anion gives the analido-phenyl complexes $TpOs(NHPh)PhCl$ (**6**) and/or $TpOs(NHPh)Ph_2$ (**7**) upon workup. In both cases, there is formation of a dark orange solution which turns bright red upon aerobic workup. Compounds **5**−**7** give mass spectra and sharp, paramagnetically shifted ^1H NMR spectra, consistent with their formulation as analogous to **4**. The X-ray structure of **5** is described in the Supporting Information.

When the reaction of **1** and PhMgBr is kept anaerobic, the initially formed dark orange intermediates can be observed,

Scheme 1

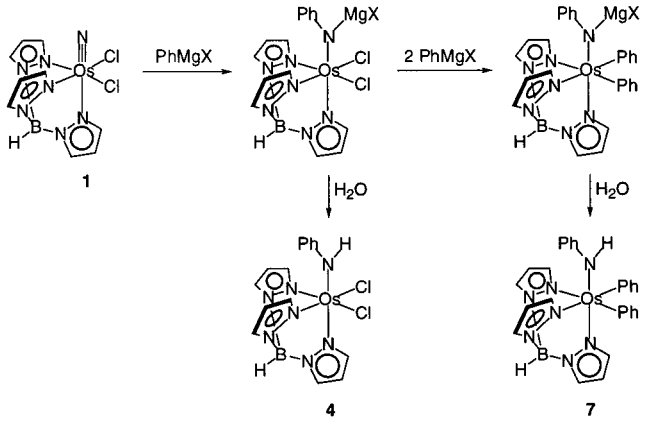

showing paramagnetic ^{1}H NMR spectra. With less than 1 equiv of Grignard reagent, a red-orange solid can be isolated that contains a mixture of **1** and a new species that has C_s symmetry and contains one Tp and one phenyl group. When excess Grignard reagent is used, the intermediate has a C_s-symmetric Tp ligand and two sets of phenyl resonances in a 2:1 ratio. Both species are very rapidly protonated by stoichiometric degassed H_2O, yielding **4** or **7** (as happens on aerobic workup). The intermediates are therefore tentatively formulated as osmium(IV) metalla-analido complexes TpOs[N(Ph)MgBr]Cl_2 (from 1 equiv of PhMgBr) and TpOs[N(Ph)MgBr]Ph_2 (from excess PhMgBr) (Scheme 1). The solubility of these species in benzene suggests that there is tight ion pairing or coordination of the imido nitrogen to the magnesium counterion, and there is likely to be oligomerization about the cation. Dark orange materials formed from PhLi have slightly different ^{1}H NMR spectra, further supporting tight bonding with the cation. Various attempts to isolate these materials, including cation exchange, have yielded only impure materials. This is due in part to their very high basicity, similar to other M−N(R)Li complexes[30] (as described elsewhere[31]).

Reactions of **1** with the alkyl carbanion sources EtMgBr, $EtAlCl_2$, $ZnEt_2$, $AlEt_3$, MeMgBr, and $PhCH_2MgBr$ give a mixture of products, predominantly ^{1}H NMR-silent materials. In two cases, with $ZnEt_2$ and MeMgBr, osmium(III) amine complexes TpOs(NH_2R)Cl_2 (R = Et, **8**; Me, **9**) have been isolated in ∼30% yields (eq 5). **8** and **9** have been characterized

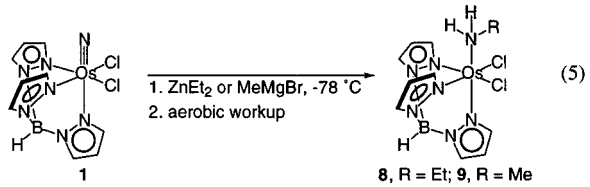

(5)

by elemental analysis, IR spectroscopy, mass spectrometry, and X-ray crystal structures (**8**, Tables 1 and 3, Figure 4; **9** (quite similar), see Supporting Information). The structures of **8** and **9** are very close to those of **4** and **5**, except that the Os^{III}−NH_2R distances of 2.129(8) (**8**) and 2.139(8) (**9**) Å are ∼0.2 Å longer than the Os^{IV}−NHAr bonds of 1.919(6) (**4**) and 1.922(7) (**5**) Å. Some reactions of **1** with 1 equiv of EtMgBr show, on protonation, small NMR signals for what is tentatively

(30) For example: (a) Dewey, M. A.; Stark, G. A.; Gladysz, J. A. *Organometallics* **1996**, *15*, 4798−4807. (b) Powell, K. R.; Pérez, P. J.; Luan, L.; Feng, S. G.; White, P. S.; Brookhart, M.; Templeton, J. L. *Organometallics* **1994**, *13*, 1851−1864.

(31) Soper, J.; Bennett, B. K.; Lovell, S.; Mayer, J. M. *Inorg. Chem.* **2001**, in press.

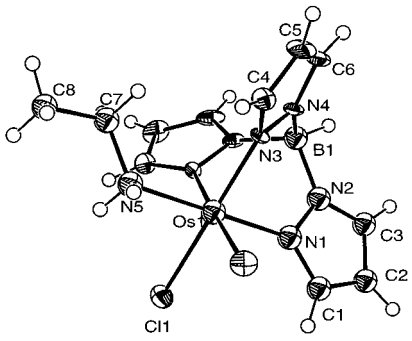

Figure 4. ORTEP diagram of TpOs(NH_2Et)]Cl_2 (**8**).

identified as the osmium(IV) amide complex TpOs(NHEt)Cl_2 (**10**; see below). Most likely, all of these reactions proceed by addition of R^- to the nitrido ligand, analogous to the aryl anion additions, but the alkyl carbanion sources cause further reduction to osmium(III). Consistent with the involvement of electron transfer, treatment of **1** with $PhCH_2MgBr$ forms substantial bibenzyl and toluene.

The nitrido-phenyl complexes **2** and **3** react very slowly with PhMgBr in THF solution at room temperature. This contrasts with the reaction of **1** with PhMgBr, which occurs instantly at 20 °C and over the course of a few hours at −78 °C. Workup of the dark brown solution from **2** + excess PhMgBr after 1 day gives ∼20% **7**, ∼20% of unreacted **2**, and NMR-silent material. The use of C_6D_5MgBr gives **7**-d_{10}, whose ^{1}H NMR spectra show that the analido phenyl ring is >95% deuterated, and the $OsPh_2$ resonances have half the intensity seen for protio-**7** (eq 6). The analogous reaction of **3** with PhMgBr over

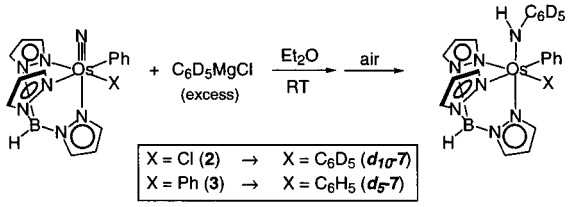

(6)

1 day gives ∼10% **7**, ∼80% unreacted **3**, and uncharacterized materials. Reaction with C_6D_5MgBr gives **7**-d_5 (eq 6), where only the analido phenyl group is deuterated (as determined by ^{1}H NMR). The use of TolMgBr in reaction 6 gives somewhat higher yields of Os(IV) analido products, apparently with analogous substitution patterns.

Reactions with Organoboranes. Anaerobic addition of BPh_3 to a toluene solution of **1** results in an immediate color change from pale orange to dark, vivid orange. Layering the solution with pentanes yields the borylamido complex TpOs[N(Ph)(BPh_2)]Cl_2 (**11**) as dark, air-sensitive orange crystals (eq 7). A

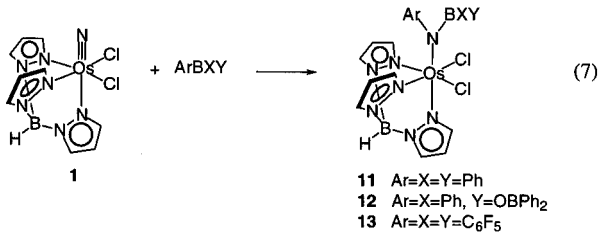

(7)

slower reaction between **1** and diphenylboronic anhydride (Ph_2BOBPh_2) forms TpOs[NPh($BPhOBPh_2$)]Cl_2 (**12**) after stirring overnight. Complex **1** reacts very rapidly with the potent electrophile $B(C_6F_5)_3$[32] in benzene to form TpOs(N(C_6F_5)[$B(C_6F_5)_2$])Cl_2 (**13**). Complexes **11**−**13** exhibit the sharp,

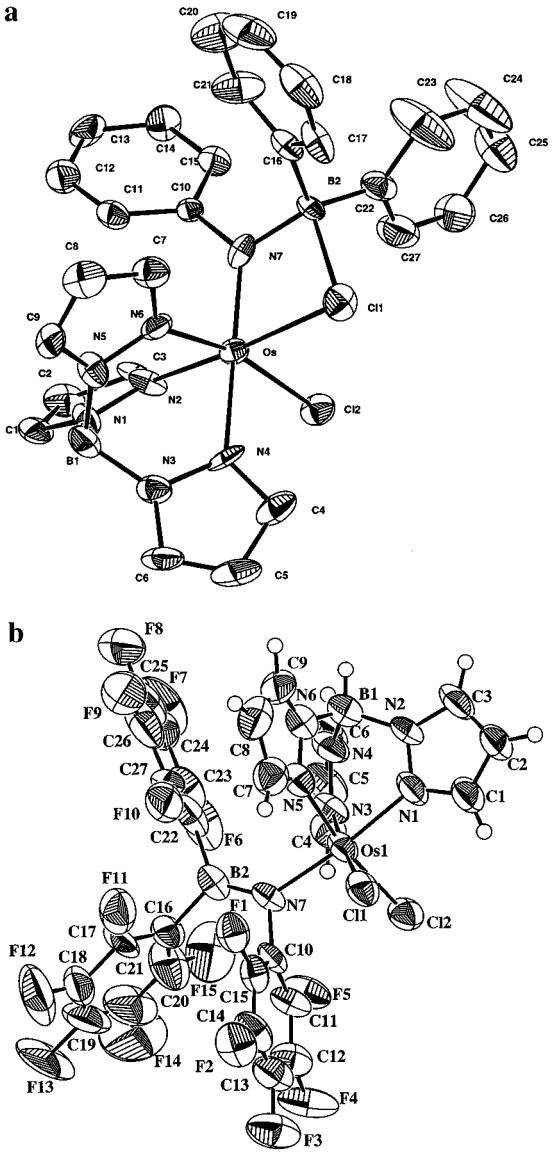

Figure 5. ORTEP diagrams of (a) TpOs[N(Ph)BPh_2]Cl_2 (**11**) and (b) TpOs(N(C_6F_5)[B(C_6F_5)$_2$])Cl_2 (**13**).

paramagnetically shifted ^{1}H NMR spectra indicative of Os(IV), with a significantly larger range of chemical shifts for **13** (for instance, one of the pyrazole peaks appears at −23.31 ppm). The paramagnetic ^{19}F NMR spectrum of **13**, though broadened such that only two peaks have resolvable F−F coupling, shows the presence of C_6F_5 groups in a 2:1 ratio.

The structures of all three compounds have been confirmed by X-ray diffraction (Tables 1 and 3, Figure 5 [for **12**, see Supporting Information]). All three show the roughly octahedral coordination about osmium typical of this group of compounds. In **11**, the boron atom forms single bonds to the nitrogen and to two phenyl groups and has an intramolecular interaction with one of the chloride ligands. At 2.078(14) Å, this is the longest B−Cl distance in the Cambridge Crystallographic Database (av 1.822 ± 0.049 Å).[24] Still, this interaction is enough to pull chloride toward the boron (N(7)−Os−B(2) = 75.7(3)°) and to lengthen the Os−Cl(1) bond (2.403(3) Å, vs Os−Cl(2), 2.355(3) Å). The boron is almost in the plane of the amide nitrogen and the ipso carbons (Σ[X-B-Y angles] = 359.2°), further indicating the weakness of the B−Cl interaction. ^{1}H NMR spectra of **11** show C_s symmetry in CD_2Cl_2 solution down to −40 °C, indicating either that there is no B−Cl interaction in solution or that the boron is rapidly "hopping" from one chloride to the other in solution. In the structures of **12** and **13** there are no B···Cl interactions, despite the higher Lewis acidity of the B(C_6F_5)$_2$ group.

Chart 1.[a]

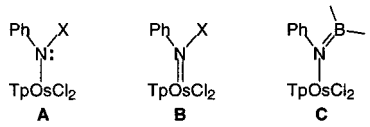

[a] X = H, B(Y)Z.

The B(2)−N(7) distances of 1.602(16) Å in **11** and 1.509(13) Å in **12** correspond to long and average B−N single bonds, respectively (average B−N, 1.52 Å[24]), while the distance of 1.408(14) Å in **13** is quite short. The osmium-amido [Os−N(7)] bond lengths vary in the reverse order: 1.884(10), 1.937(7), and 2.057(7) Å for **11**−**13** (compare Os−N7 in **4** of 1.919(6) Å). In [Os(en_{-H})$_2$(en)]Br_2 (en_{-H} = $H_2NCH_2CH_2NH^-$), the Os−N(amide) bonds of 1.896(7) Å are much shorter than the Os−N(amine) distances (cis, 2.113 (9); trans, 2.194(7) Å), and this has been attributed to Os−N π bonding.[33] On this basis, there is likely to be significant Os−N π bonding in **11** and **12**, with a large contribution of resonance form **B** in Chart 1. In **11**, the B−Cl interaction reduces the contribution of **C**, leading to shorter Os−N and longer N−B distances. Complex **13** is best described by **C**, a result of electron-withdrawing C_6F_5 groups. **C** is also the best description of the bonding for the two previous reports of borylamido complexes, bulky M[N(Ar)(BAr_2)]$_2$ compounds reported by Power et al.[34] and bis(borylamide) complexes described by Schrock et al.[35]

Exposure of **11**−**13** to air, or addition of water under oxygen-free conditions, results in hydrolysis of the B−N bonds to form the analido complexes **4** or TpOs(NHC_6F_5)Cl_2 (**14**; eq 8). In

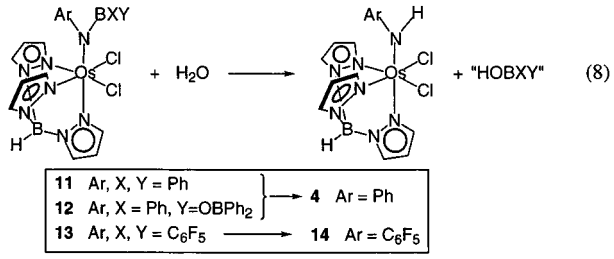

the case of **11**, the boron hydrolysis product is Ph_2BOBPh_2, as determined by ^{1}H NMR. **11** and **13** are very sensitive to atmospheric moisture, even in the solid state, while solid **12** can be handled briefly in the air. ^{1}H and ^{19}F NMR spectra of **14** are paramagnetically shifted, with pyrazoles in the expected 2:1 ratio and shifted but unbroadened fluorine resonances.

Complex **1** reacts rapidly with tri(tolyl)borane to give TpOs[N(Tol)($BTol_2$)]Cl_2 (as determined by ^{1}H NMR), which hydrolyzes to TpOs(NHTol)Cl_2 (**5**). Reacting **1** with a 10-fold excess of both $BTol_3$ and BPh_3 gave a 1:1.4 ratio of TpOs[N(Tol)($BTol_2$)]Cl_2 to **11** and roughly the same ratio of **5**:**4** on hydrolytic workup. ^{1}H NMR spectra of the reaction mixture of **1** plus $BTol_3$ and BPh_3 showed no evidence of the crossover products TpOs[N(Ph)($BTol_2$)]Cl_2 and TpOs[N(Tol)(BPh_2)]Cl_2 (<10%). Reac-

(32) Piers, W. E.; Chivers, T. *J. Chem. Soc. Rev.* **1997**, *26*, 345−354.

(33) Lay, P. A.; Sargeson, A. M.; Skelton, B. W.; White, A. H. *J. Am. Chem. Soc.* **1982**, *104*, 6161−6162.

(34) Chen, H.; Bartlett, R. A.; Olmstead, M. M.; Power, P. P.; Shoner, S. S. *J. Am. Chem. Soc.* **1990**, *112*, 1048−1055.

(35) Warren, T. H.; Schrock, R. R.; Davis, W. M. *Organometallics* **1996**, *15*, 562−569.

tion with the unsymmetrical $BPh(Tol)_2$ suggested that the crossover products would have been resolvable. There is thus no scrambling of N−aryl or B-aryl groups either during or after the reaction. The reaction of **1** with $BPh(Tol)_2$ gave, after hydrolysis, a 7:1 ratio of **5**:**4**. In a similar competition study, $B(C_6F_5)_3$ and BPh_3 were mixed 1:1 in $CDCl_3$ (there was no evidence of exchange over 3 h), and 0.33 equiv of **1** was added. Prompt analysis by ^1H and ^{19}F NMR showed only **11** and unreacted BPh_3 and $B(C_6F_5)_3$, and aerobic workup gave **4** in good yield.

Complex **1** also reacts rapidly with $BPhCl_2$ to give a complex similar to **11** and **12**, as determined by ^1H NMR. Hydrolysis yielded primarily **4**, with small amounts of ^1H NMR-silent materials. Complex **1** does not react with 2-phenyl-1,3,2-dioxaborinane, $Ph[BOCH_2CH_2CH_2O]$, even after 3 days at 70 °C in benzene solution. Heating a solution of **1** and excess $NaBPh_4$ in acetonitrile results in a very slow reaction with some formation of **4**. This suggests the presence of trace water and that the reaction could have proceeded by initial hydrolysis of the BPh_4^- to BPh_3.

The alkylboranes BEt_3 and $BEt_2(OMe)$ also add to **1**, forming $TpOs[N(Et)B(Et)X]Cl_2$ (X = Et, **15**; OMe, **16**; eq 9). BEt_3 reacts

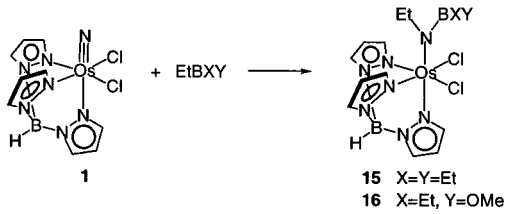

(9)

rapidly, while $BEt_2(OMe)$ requires over 40 min at room temperature to form **16**. The same reactivity pattern is observed for arylboranes: BAr_3 reacts faster than Ph_2BOBPh_2. The products are assigned on the basis of their ^1H NMR spectra, both showing standard C_s symmetry pyrazole resonances and two types of ethyl groups. The ethyl groups bound to boron are broadened by the quadrupolar boron nucleus (as observed in free ethyl boranes), but the ethyl groups bound to nitrogen show a clear triplet/quartet pattern. A few resonances are shifted out of the diamagnetic region. The FAB/MS of **15** shows a weak parent ion with stronger signals due to M^+-BEt_2 and M^+-BEt_2Cl. Brief atmospheric exposure of **16** in $CDCl_3$ gives clean conversion to $TpOs(NHEt)Cl_2$ (**10**), which has been observed in low yield in the reaction of **1** with EtMgCl (see above). It has been characterized by its mildly paramagnetically shifted ^1H NMR spectrum with C_s symmetry and one ethyl group, and its FAB mass spectrum (M^+, $M^+ - Cl$). In contrast, **15** decays in the air without formation of new ^1H NMR-active Tp species.

The diphenyl nitrido complex **3** rapidly adds $B(C_6F_5)_3$, forming a green complex even as the methylene chloride solvent is thawing. The product is the Lewis acid adduct $TpOs[NB(C_6F_5)_3]Ph_2$ (**17**; eq 10), in which the nitrido ligand simply binds to the boron without insertion into a B−C bond. Exposure of

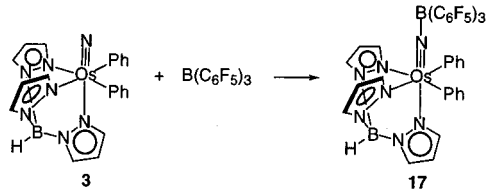

(10)

17 to the atmosphere results in rapid conversion back to **3**. In contrast, BPh_3 reacts with $TpOs(N)Ph_2$ (**3**) in benzene only over

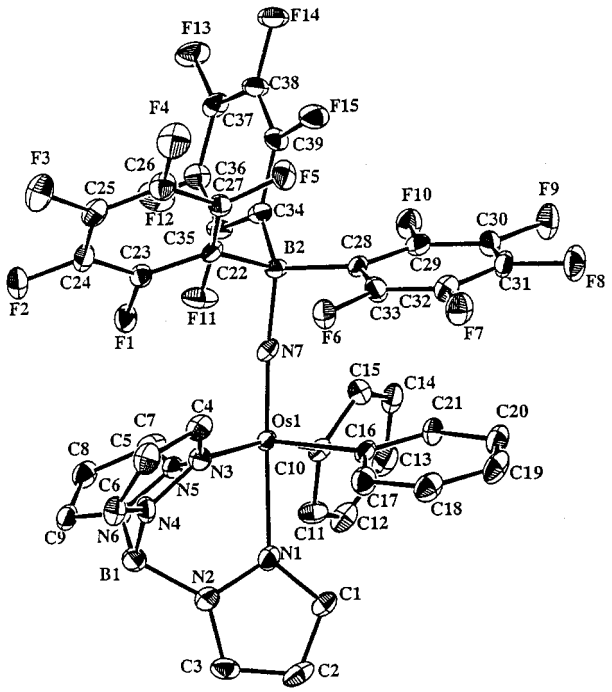

Figure 6. ORTEP diagram of $TpOs[NB(C_6F_5)_3]Ph_2$ (**17**).

the course of several days at room temperature, and ^1H NMR spectra of the resulting purple solution show only the disappearance of starting material. No products analogous to **11** or **17** are observed.

Complex **17** has a ^1H NMR spectrum indicative of a diamagnetic complex, consistent with the Os(VI) formulation. The equivalence of pairs of pyrazole and phenyl groups shows C_s symmetry. Only the chemical shifts of the trans pyrazole are dramatically shifted from **3**, as expected from perturbation of the nitrido ligand. The similarity of the spectra shows that the phenyl groups remain on the osmium. ^{19}F NMR indicates the presence of only one type of C_6F_5 group, and the chemical shift of −81.6 ppm for the para fluorine atoms is strongly suggestive of an adduct.[36] The X-ray structure of **17** (Tables 1 and 2, Figure 6) confirms the formulation. As is typical of nitrido-borane adducts,[1,37] the Os−N(7) bond (1.688(3) Å) is only slightly lengthened from that in **3** (1.634(4) Å). The B(2)−N(7) bond length (1.591(5) Å) is a long B−N single bond (see above). There is a π stacking interaction (~3.2 Å) between one of the C_6F_5 groups on the boron and one of the C_6H_5 groups on the metal center. The Os−N−B angle (167.7(3)°) is slightly bent, apparently to accommodate this interaction. While $B(C_6F_5)_3$ and $TpOs(N)Ph_2$ (**3**) could both be considered fairly bulky, the presence of the intervening nitrogen leads to an Os−B distance of 3.26 Å and little steric interaction.

Ab Initio Studies of $TpOs(N)Cl_2$ (1) and $TpOs(N)Me_2$ (18). Ab initio calculations have been performed on **1** and the hypothetical dimethyl analogue $TpOs(N)Me_2$ (**18**). The calculations were done prior to our obtaining an X-ray structure of **1**, so the coordinates of the related $TpTc(O)Cl_2$[38] were used as a

(36) Massey, A. G.; Park, A. J. *J. Organomet. Chem.* **1966**, *5*, 218−225.

(37) Ritter, S.; Abram, U. *Inorg. Chim. Acta* **1995**, *231*, 245−248. (b) Ritter, S.; Abram, U. *Z. Anorg. Allg. Chem.* **1996**, *622*, 965. (c) Datona, R.; Schweda, E.; Strähle, J. *Z. Naturforsch. B* **1984**, *39*, 733−736. (d) Yoshida, T.; Adachi, T.; Yabunouchi, N.; Ueda, T.; Okamoto, S. *J. Chem. Soc., Chem. Commun.* **1994**, 151−152. (e) Bishop, M. W.; Chatt, J.; Dilworth, J. R.; Dahlstrom, P.; Hyde, J.; Zubieta, J. *J. Organomet. Chem.* **1981**, *213*, 109−124.

(38) Thomas, R. W.; Estes, G. W.; Elder, R. C.; Deutsch, E. *J. Am. Chem. Soc.* **1979**, *101*, 4581.

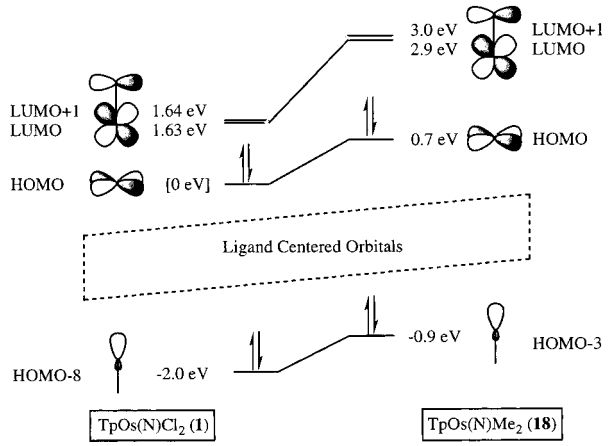

Figure 7. Partial molecular orbital diagram for $TpOs(N)Cl_2$ (**1**) and $TpOs(N)Me_2$ (**18**), from Xα/LANL2DZ/RHF/LANL2MB calculations. Energies are given relative to the HOMO of **1**.

starting point. The molecular geometry was optimized at the RHF/LANL2MB level of theory, with imposed C_s symmetry. For **18**, the computed structure of **1** was used to start, with Os−C bonds of 2.15 Å. There is reasonably good agreement between the computed structure and the X-ray results (Table 2), although the computations underestimate the trans effect of the nitrido ligand and give an overly long Os−Cl distance. Calculations on the simpler $[Os(N)X_4]^-$ complexes (X = Cl,[39] Me[40]) show similar discrepancies at this level of theory but better agreement upon optimization at the Xα/LANL2DZ level (see Supporting Information). The differences between the computational and crystallographic structures of **1** and **18** should have little effect on the orbital energies and compositions. These orbital properties were determined by single-point calculations at the optimized geometries at the Xα/LANL2DZ level.

The HOMO in both **1** and **18** is a mixture of the Os d_{xy} orbital and Cl or C p orbitals. It is of δ symmetry with respect to the nitrido ligand and roughly nonbonding, as drawn in Figure 7. The orbital energies in this figure are given relative to the HOMO of **1**; similar energy spacings (though not absolute energies) were observed in RHF calculations. The orbitals below the HOMO are primarily ligand centered; notable are the nitrogen lone pair orbital and the Os≡N π orbitals (the HOMO-8 and HOMO-15,16 in **1**). The LUMO and nearly degenerate LUMO + 1 in both **1** and **18** are the Os−N π* orbitals, one in the *xz* plane and one in the *yz* plane. Each is primarily an out-of-phase combination of an osmium π-symmetry d orbital, d_{xz} or d_{yz}, and the corresponding nitrogen p orbital, p_x or p_y (illustrated for **1** in Figure 8). These results fit the widely accepted Ballhausen and Gray d-orbital splitting pattern for pseudo-octahedral complexes with one multiply bonded ligand.[1a,41] The remarkable feature is the large amount of nitrogen character in the LUMO and LUMO + 1, roughly comparable to the amount of osmium d character. Thus, it is not surprising that an entering nucleophile will attack at nitrogen. The orbital pattern, with accessible π* LUMOs and low-energy lone pair and π orbitals, resembles that of CO.

The frontier orbital energies of **1** are lower than those of **18**, a result of the lesser donating character of chloride vs methyl.

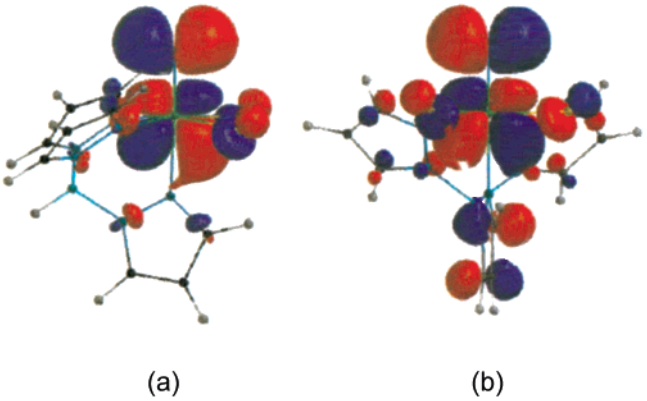

Figure 8. Plots of the LUMO (a) and LUMO + 1 (b) of $TpOs(N)Cl_2$ (**1**), from Xα/LANL2DZ/RHF/LANL2MB calculations.

This is illustrated by the 0.7 eV lower HOMO (d_{xy}) orbital energy in **1**. The predominantly nitrogen lone pair orbital in **1** (the HOMO-8) is 1 eV lower in energy and has less frontier orbital character than the equivalent orbital (the HOMO-3) in **18**. The difference is even larger for the LUMO/LUMO + 1, with those in **1** being 1.3 eV lower. This means that the HOMO/LUMO gap is smaller in **1** than in **18** (1.6 vs 2.2 eV). Even larger differences in orbital energies are observed when comparing $[Os(N)Cl_4]^-$ vs $[Os(N)Me_4]^-$ because four ligands are different instead of two, as in **1** vs **18** (see Supporting Information). These energetic differences are not apparent in the composition of the LUMOs: even for **18** the π^* orbitals have substantial nitrogen character.

Discussion

The additions of Grignard reagents and aryl boranes to the Os(VI) nitrido complex $TpOs(N)Cl_2$ (**1**) are novel. The nitrido ligand is formally a closed-shell anion and would normally be expected to add electrophiles, not nucleophiles. There is much interest in exploiting such a reversal of nitrogen reactivity.[7]

I. The Mechanism of Grignard Addition to the Nitrido Ligand. The reaction of **1** with 1 equiv of PhMgBr initially generates a dark orange material, indicated to be the osmium(IV) complex $[TpOs(NPhMgCl)Cl_2]$ (Scheme 1). It is a more reactive version of the borylamido complexes **11**−**13**. Both can be viewed as having a very basic $TpCl_2Os^{IV}{=}NR^-$ fragment that is strongly stabilized by a Lewis acidic $MgCl^+$ or BX_2^+ fragment. They are better described as metalla-analido rather than imido complexes. Osmium(IV) imido complexes without an associated cation would be rare examples of d^4 octahedral imido complexes,[42] in which two electrons formally occupy OsN π* orbitals (the LUMOs in **1**).[1] The antibonding interaction should be minimized on decreasing the Os−N−Ph angle and binding a cation to this electron pair.

The key issue is how the C−N bond is formed. Three possible mechanisms have been considered (Scheme 2). Path I involves an initial electron transfer to generate a phenyl radical and $[TpOs(N)Cl_2^{\bullet-}]$, followed by trapping of the phenyl radical to give the observed intermediate. Grignard reagents often react by initial electron transfer, and rapid radical trapping is well

(39) Phillips, F. L.; Skapski, A. C. *J. Cryst. Mol. Struct.* **1975**, *5*, 83−92.

(40) Chosen as a computational model for $[Os(N)(CH_2SiMe_3)_4]^-$: (a) Belmonte, P. A.; Own, Z.-Y. *J. Am. Chem. Soc.* **1984**, *106*, 7493−7496. (b) Shapley, P. A.; Own, Z.-Y.; Huffman, J. C. *Organometallics* **1986**, *5*, 1269−1271.

(41) Balhausen, C. J.; Gray, H. B. *Inorg. Chem.* **1962**, *1*, 111.

(42) Wigley, D. E. *Prog. Inorg. Chem.* **1994**, *42*, 239−482. (b) Coia, G. M.; Devenney, M.; White, P. S.; Meyer, T. J.; Wink, D. A. *Inorg. Chem.* **1997**, *36*, 2341−2351 and references therein. (c) Arndtsen, B. A.; Sleiman, H. F.; Chang, A. K.; McElwee-White, L. *J. Am. Chem. Soc.* **1991**, *113*, 4871−4876. (d) Au, S.-M.; Huang, J.-S.; Yu, W.-Y.; Fung, W.-H.; Che, C.-M. *J. Am. Chem. Soc.* **1999**, *121*, 9120−9132. (e) Reference 31. (f) d^4-Rhenium imido−alkyne complexes have nonoctahedral structures with a different electronic structure: Williams, D. S.; Schrock, R. R. *Organometallics* **1993**, *12*, 1146−1160.

Scheme 2

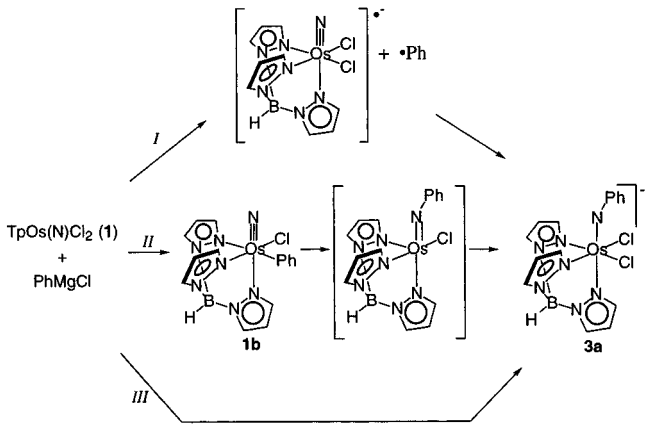

precedented for metal−oxo complexes.[43] Complex **1** can be reduced, albeit at low potentials ($E_{red} = -0.98$ vs SSCE).[16c,23] However, this pathway can be easily ruled out for the present reactions because the reaction proceeds in high yield in THF solvent, a good trap for Ph• ($k = 4.8 \times 10^6$ M^{-1} s^{-1}).[44] An osmium species of concentration $\leq 10^{-4}$ M would have to react with Ph• with an impossible rate constant of $\geq 10^{12}$ M^{-1} s^{-1}, faster than the diffusion limit, to compete with trapping by 12.3 M THF solvent.

Path II involves initial phenyl addition to the osmium center to form **2**, followed by [1,2] phenyl migration to nitrido ligand. Phenyl migration to an oxo ligand has been observed for a related rhenium(VII) oxo complex.[21a] However, this pathway involves trapping a coordinatively unsaturated intermediate with Cl^-, and no bromide incorporation is observed when PhMgBr is used. To more rigorously test for the intermediacy of metal−aryl complexes, TpOs(N)(Ph)Cl (**2**) and TpOs(N)$(Ph)_2$ (**3**) were synthesized. Both species are stable, even at elevated temperatures, with no evidence for aryl migration. Reactions of **2** or **3** with excess PhMgBr-d_5 give partially deuterated **7** in low yield, but the reactions are much slower than the reaction of **1** under the same conditions. In addition, the protio phenyl group remains on the osmium, indicating that aryl migration does not occur in the formation of **7**. Complexes **2** and **3** are not kinetically or mechanistically competent to be intermediates, ruling out path II. Intermediacy of a seven-coordinate species [TpOs(N)$Ph_{3-x}Cl_x^-$] ($x = 0-2$) seems unlikely,[45] and it would have to have nonexchanging phenyl groups.

The data indicate a mechanism of direct addition of the carbanion to the nitrido ligand (path III). We know of no clear precedent for such a carbanion addition to a nitrido, oxo, imido, or sulfido ligand. This reaction is, however, well known for carbene and carbonyl ligands.[46] A recently reported reaction proceeds by direct attack of LiMe at a selenido ligand bound to tantalum.[47] In the microscopic reverse of this mechanism, Schrock et al. have suggested that an unobserved intermediate [N_3N]M−P(Li)Ph complex eliminates LiPh to give the terminal phosphido complexes, [N_3N]M≡P ([N_3N] = $(Me_3SiNCH_2CH_2)_3N$; M = Mo, W).[48] Hydride addition to an electrophilic imido ligand occurs via initial attack at a carbonyl ligand.[49]

II. The Mechanism of Arylboron Addition to the Nitrido Ligand. The insertion of the nitrido ligand of **1** into B−C bonds (reactions 7 and 9) is, to our knowledge, without precedent for any metal−ligand multiple bond. A number of organo- and haloboranes form Lewis acid adducts with nitrido complexes, such as Re$(NBPh_3)(Et_2dtc)_2(PMePh_2)$ (Et_2dtc = diethyldithiocarbamate) and TpOs[$NB(C_6F_5)_3$]Ph_2 (**17**).[1,37] But these reactions do not transfer a boron substituent to nitrogen. Close analogies to reactions 7 and 9 are the insertion of nitrogen into B−C bonds by chloramines and related reagents (eq 11),[50] and C → N migration of R groups in the Hoffman rearrangement.[51] Reaction

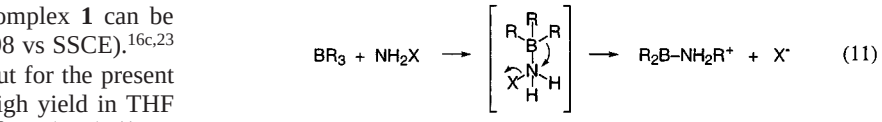

11 occurs by [1,2] migration of R^- from boron to nitrogen, with displacement of the N−X bonding electrons to give X^- (Cl, OSO_3H, etc.). The relative rates of arylborane addition to **1** support a similar mechanism of R^- migration, with two electrons displaced from an Os−N π bond to the Os center. The reaction of B$Ph(Tol)_2$ shows that, in a direct intramolecular competition, tolyl is 3.5 times more likely to be transferred to nitrogen than phenyl (after statistical correction). Preferential transfer of the more electron-rich group is characteristic of carbanion migrations to an electron-deficient center.[51] Almost all organic and organometallic [1,2] migrations are of this type.[50,51] [1,2] Migrations of R^- are symmetry allowed, while R^+ moving to an electron pair is formally forbidden.[51]

In contrast to the preference for tolyl over phenyl migration with B$Ph(Tol)_2$, the *inter*molecular competition of BPh_3 with B$(Tol)_3$ shows a small preference for phenyl over tolyl migration. This shows that the products are not simply determined by migratory aptitudes and indicates a multistep mechanism. The same conclusion is derived from the large variation in rates of phenylborane additions: BPh_3 (within seconds) > Ph_2-$BOBPh_2$ (stirring overnight) > Ph[O(BOCH$_2$CH$_2$CH$_2$O] (unreactive over 3 days at 70 °C). This is too big an effect to solely reflect changes in the nucleophilicity of the Ph−B bonds. It indicates that the Lewis acidity of the boron plays a key role. This accounts for the rapid reaction of **1** with B$(C_6F_5)_3$, almost as fast as that with BPh_3: the very high Lewis acidity of B$(C_6F_5)_3$ compensates for C_6F_5 being a much poorer migrator than C_6H_5.

The data indicate a stepwise mechanism (Scheme 3) involving reversible formation of an initial borane adduct **A**, followed by [1,2] migration of R^- to an electrophilic nitrogen, similar to eq 11. The reaction with B$Ph(Tol)_2$ reflects the relative rates only

(43) Cook, G. K.; Mayer, J. M. *J. Am. Chem. Soc.* **1994**, *116*, 1855−1868 and references therein.

(44) Scaiano, J. C.; Stewart, L. C. *J. Am. Chem. Soc.* **1983**, *105*, 3609−3614.

(45) While there are precedents for seven-coordinate transition metal Tp complexes, examples seem to be restricted to larger metal centers, such as Os^{I} and Os^{II} (Trofimenko, S. *Chem. Rev.* **1993**, *93*, 943−980. Burns, I. D.; Hill, A. F.; White, A. J. P.; Williams, D. J.; Wilton-Ely, J. D. E. T. *Organometallics* **1998**, *17*, 1552−1557), and these are often fluxional. For related Re^{V}−oxo complexes with the $B(pz)_4^-$ ligand, there is a preference for dissociating a pyrzole rather going seven-coordinate (Paulo, A.; Domingos, A.; Santos, I. *Inorg. Chem.* **1996**, *35*, 1798−1807).

(46) Collman, J. P.; Hegedus, L. S.; Norton, J. R.; Finke, R. G. *Principles and Applications of Organotransition Metal Chemistry*; University Science Books: Mill Valley, CA, 1987; pp 401−406.

(47) Shin, J. H.; Parkin, G. *Organometallics* **1995**, *14*, 1104.

(48) Mösch-Zanetti, N. C.; Schrock, R. R.; Davis, W. M.; Wanninger, K.; Seidel, S. W.; O'Donoghue, M. B. *J. Am. Chem. Soc.* **1997**, *119*, 11 037−11 048.

(49) Luan, L.; Brookhart, M.; Templeton, J. L. *Organometallics* **1992**, *11*, 1433−1435.

(50) Brown, H. C. *Organic Synthese via Boranes*; Wiley: New York, 1975. (b) Matteson, D. S. *Stereodirected Synthesis with Organoboranes*; Springer: New York, 1995; pp 48−57. (c) Onak, T. *Organoborane Chemistry*; Academic Press: New York, 1975; pp 100−101, 106. (d) Kabalka, G. W.; Wang, Z. *Organometallics* **1989**, *8*, 1093−1095.

(51) March, J. *Advanced Organic Chemistry*, 4th ed.; Wiley: New York, 1992; discussions of [1,2] migrations, p 1051ff (see also ref 21a); Hoffman rearrangment, pp 1090−1091.

Scheme 3[a]

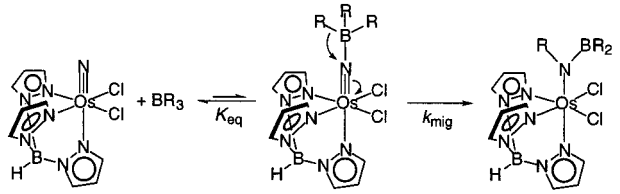

[a] Rate = $K_{eq}k_{mig}$[TpOs(N)Cl_2][BR_3].

of the migration step. In the *inter*molecular competition, however, the faster tolyl migration step is more than balanced by the stronger pre-equilibrium binding of the more Lewis acidic BPh_3. An alternative mechanism of concerted, direct attack of the B−C bond at nitrogen does not account for the role of the boron Lewis acidity. Initial interaction of the electrophilic nitrogen with the aromatic ring is conceivable for the arylboranes but is inconsistent with the facile reaction with ethylboranes. (Initial phenyl transfer from boron to osmium is unlikely, given the experiments described above with Grignard reagents and the low reactivity of **3**.)

The characterization of the borane adduct TpOs[NB(C_6F_5)$_3$]-Ph_2 (**17**) provides further support for Scheme 3, as it is an excellent model for the initial borane adduct **A**. Such adducts are not observed for **1**, both because they react further and because **1** is an unusually weak nucleophile (it is inert to BF_3·Et_2O, MeOTf, and [Ph_3C][BF_4] at ambient temperatures). TpOs-(N)Ph_2 (**3**) is a much better nucleophile, favoring the initial equilibrium formation of **17**. And the lower electrophilicity of **3** inhibits the aryl migration step, allowing observation of **17**. In a related reaction, an adduct has been observed between B(C_6F_5)$_3$ and a bis(amino)silylene prior to migration of C_6F_5 from B to Si.[52]

III. Electrophilic and Nucleophilic Character of the Nitrido Ligand. Nitrido ligands can show nucleophilic and/or electrophilic character.[1,53,54] The dominant reactivity of **1** is as an electrophile, adding Ph^- from PhMgX and BPh_3 (and adding PPh_3[25]). Meyer and co-workers have elegantly shown the electrophilicity of **1** and related Os(VI) nitrido complexes, for instance by their addition of amines and phosphines.[55] In contrast, the diphenyl derivative TpOs(N)Ph_2 (**3**) is a poor electrophile, reacting only slowly with PhMgCl and PPh_3.

The DFT calculations provide insight into the reactivity of the nitrido ligand and how it is tuned by the ancillary ligands. In **1**, the nearly degenerate LUMO and LUMO + 1 (Os−N π^* orbitals) are low in energy and have substantial nitrogen character. These orbitals are higher in energy in the dimethyl complex **18**, used as a computational model for the diphenyl complex **3**. This is the reason for the higher electrophilicity of **1** versus **2** and **3** (and **18**). Conversely, the nitrogen lone pair is higher and closer to the HOMO in **18** (Figure 7), consistent with **3** forming a stable adduct with B(C_6F_5)$_3$, while **1** has very low nucleophilicity. These trends are mirrored in the redox potentials: adding hydrocarbyl ligands makes reduction substantially more difficult [−1.35 (**1**), −1.89 (**2**), −2.04 (**3**) V] and oxidation much more facile [∼2.05 (**1**), 1.60 (**2**), 1.36 (**3**) V vs $Cp_2Fe^{+/0}$ in MeCN].[23] The pattern of higher electrophilicity for halide vs organometallic derivatives has been observed previously, such as in electrophilic [Os(N)Cl_4]$^-$ vs nucleophilic [Os(N)(CH_2SiMe_3)$_4$]$^-$ (which is harder to reduce by a remarkable 1.45 V).[8] Calculations on these compounds are in general agreement with the results given here.[12]

It is interesting in this context to consider the analogy between **1** and CO, advanced when **1** was observed to act as a π acid ligand for late transition metals.[56] Both **1** and CO have low-lying LUMOs of π symmetry and low nucleophilicity. CO inserts into B−C bonds of organoboranes much like **1**, and a similar mechanism is proposed, with alkyl group migration from B to C occurring in an initial CO−borane adduct.[57] It seems likely that the reactions of **1** with BR_3, ArMgX, and ArLi all proceed through an initial N−M adduct. Binding of the Lewis acid to the nitrido ligand increases its electrophilicity, facilitating the migration. The strategy of enhancing the electrophilic reactivity of nitrido ligands by binding Lewis acids has been employed by a number of groups[1,5a,b,58] and is also well established for carbon monoxide.

IV. Implications: Reactions at Ligands. The reactions of **1** occur predominantly at the nitrido ligand and not at osmium. In a direct comparison, external addition of Ph^- to **1** is facile, while [1,2] phenyl migration from Os to N in **2** and **3** does not occur. Both pathways involve adding Ph^- to the multiply bonded ligand—why is external attack favored? One reason is that the phenyl group in PhMgX or PhLi is a better nucleophile than an osmium-bound phenyl group. Perhaps more importantly, the presence of a phenyl ligand on osmium strongly decreases the electrophilicity of the nitrido ligand (see above). And in the cases described here, binding of a Lewis acid enhances the electrophilicity of the multiple bond.

These ideas suggest that direct addition of carbanions and other good nucleophiles to metal−ligand multiple bonds (eq 12) is likely to be more facile than initial addition to the metal followed by migration. Preference for direct attack is frequently

$$L_nM{\equiv}E + R^- \longrightarrow [L_nM{-}E{-}R]^- \qquad (12)$$

seen in the more developed literature on metal carbonyl complexes. For instance, CpRe(CO)(NO)Cl reacts with hard, nucleophilic sources of Ph^- directly at the electrophilic carbonyl to produce an anionic acyl complex. The related phenyl complex CpRe(CO)(NO)Ph, prepared by chloride metathesis using the softer phenylcuprate, does not undergo phenyl migration to CO.[59] This system is closely analogous to the reactivity of **1** with Ph^- sources. If the preference for direct attack over metathesis/migration is general, re-examination of the reactions of V(O)Cl_3 with arylmercury compounds[60] and Cr(N^{t}butyl)$_2$-($OSiMe_3$)$_2$ with $ZnPh_2$[61] may be warranted. In both cases [1,2] migration was suggested, but direct attack at the multiple bond is a good alternative. Direct attack may be occurring in many other systems, such as the alkylation of OsO_4 with (Me_3SiCH_2)$_2$-

(52) Metzler, N.; Denk, M. *Chem. Commun.* **1996**, 2657−2658.
(53) Cf., Mo(N)(tetraphenylporphyrin): Kim, J. C.; Lee, B. M.; Shin, J. I. *Polyhedron* **1995**, *14*, 2145−2149.
(54) Electrophilic reactivity of oxo ligands: (a) Holm, R. H. *Chem. Rev.* **1987**, *87*, 1401−1449. (b) Mayer, J. M. *Adv. Trans. Met. Coord. Chem.* **1996**, *1*, 105−157. (c) Seymore, S. B.; Brown, S. N *Inorg. Chem.* **2000**, *39*, 325−332.
(55) Huynh, M. H. V.; El-Samanody, E.-S.; Demadis, K. D.; White, P. S.; Meyer, T. J. *Inorg. Chem.* **2000**, *39*, 2825−2830 and references therein. (b) Reference 16.
(56) Crevier, T. J.; Lovell, S.; Mayer, J. M. *J. Chem. Soc., Chem. Commun.* **1998**, 2371−2372.
(57) Onak, T. *Organoborane Chemistry*; Academic Press: New York, 1975. (b) Hillman, M. E. D. *J. Am. Chem. Soc.* **1962**, *84*, 4715.
(58) Shapley, P. A.; Shusta, J. M.; Hunt, J. L. *Organometallics* **1996**, *15*, 1622−1629.
(59) Sweet, J. R.; Graham, W. A. G. *J. Organomet. Chem.* **1983**, *241*, 45−51.
(60) Reichle, W. T.; Carrick, W. L. *J. Organomet. Chem.* **1970**, *24*, 419−426. (b) Thiele, V. K. H.; Schumann, W.; Wagner, S.; Brüser, W. *Z. Anorg. Allg. Chem.* **1972**, *390*, 280−288.
(61) Nugent, W. A.; Harlow, R. L. *J. Am. Chem. Soc.* **1980**, *102*, 1759−1760.

Mg to give $Os(O)(CH_2SiMe_3)_4$.[62] Finally, it should be noted that the preference for direct attack observed here is consistent with the recent conclusion that the cis-hydroxylation of olefins by OsO_4 proceeds via olefin attack at oxygen, rather than involving a 1,2 alkyl migration.[9]

The insertion of a nitrido ligand into B−C bonds (eqs 7 and 9) is an interesting example of a reaction that occurs at a ligand. This reaction resembles oxidative addition and σ-bond metathesis processes in that an X−Y bond is cleaved and the X and Y fragments are added to the metal complex. In oxidative addition, both X and Y bind to the metal center with concomitant oxidation of M. In σ-bond metathesis, X is added to the metal and Y is added to a ligand, without redox change at the metal. In reactions 7 and 9, both the R and BX_2 pieces are added to the nitrido ligand, and the osmium is formally reduced by two electrons. Current work is exploring the scope of such reactions that occur at ligands, without change in the atoms bound to the metal center.

Conclusions

The osmium(VI) nitrido complex $TpOs(N)Cl_2$ (**1**) is electrophilic at nitrogen but is a poor nucleophile. PhMgCl and related reagents deliver carbanions directly to the nitrido ligand to form reactive metalla-analido complexes which are readily protonated to analido complexes such as $TpOs(NHPh)Cl_2$ (**4**). These reactions proceed by direct addition of R^- to the nitrido ligand, and not via osmium−carbon bonded intermediates such as TpOs(N)PhCl (**2**). Independently prepared **2** and $TpOs(N)Ph_2$ (**3**) add external C_6D_5MgCl at nitrogen, without migration of osmium-bound phenyl groups. A mechanism of electron transfer from PhMgCl to **1**, forming $Ph^{\bullet}$, is ruled out by the lack of trapping of the radical by THF solvent. Reactions of **1** with alkyl- and arylboranes similarly result in transfer of one organic group to nitrogen, leading to isolable borylamido complexes such as $TpOs[N(Ph)(BPh_2)]Cl_2$ (**11**). This is an unprecedented insertion of a nitrido ligand into a boron−carbon bond. The mechanism proposed involves pre-equilibrium formation of a nitrido-borane adduct, followed by a 1,2 shift of an organic group from boron to nitrogen (Scheme 3). A related adduct, $TpOs[NB(C_6F_5)_3]Ph_2$ (**17**), has been structurally characterized. The mechanism is supported by the strong influence of both the electrophilicity of the borane and the nucleophilicity of the migrating group. Similar mechanisms have been proposed in related reactions of organoboranes with chloramines, azides, and CO. The unusual reactivity of **1**, and the much diminished reactivity of **3**, are consistent with the orbital picture derived from ab initio calculations. The electrophilicity of **1** derives from its accessible LUMO and LUMO + 1, which are Os−N π^* orbitals with significant density on the nitrogen. The lone pair on the nitrido ligand in **1** is the low-lying HOMO-8. This bonding scheme and reactivity have similarities to those of CO. The reactions described here are interesting examples of metal-mediated chemistry that occurs with bond making and bond breaking at ligands, without change in the atoms bound to the metal center.

Experimental Section

General Considerations. All manipulations were conducted in the absence of air and water using dried reagents and glovebox and high-vacuum techniques, except where noted. ^1H NMR spectra were recorded on Bruker AC-200, AF-300, AM-499, and WM-500 spectrometers at ambient temperatures and referenced to Me_4Si or residual solvent peaks: δ (multiplicity, coupling constant, number of protons, assignment). All pyrazole J_{HH} couplings are 2 Hz. ^{13}C NMR spectra were recorded on Bruker AC-200 and AF-300 spectrometers at ambient temperatures and referenced to the solvent. ^{19}F chemical shifts were recorded at 188 MHz and are reported in ppm with CF_3COOH used as an external reference. IR spectra were obtained as thin films or Nujol mulls on NaCl plates using a Perkin-Elmer 1600A spectrometer and are reported in wavenumbers. Each complex contains a number of stretches associated with the Tp ligand that typically vary by less than 3 wavenumbers: 3112 (m), 1503 (m), 1404 (s), 1312 (s), 1216 (s), 1118 (s), 1075 (m), 1046 (vs), 982 (w), 768 (s), 715 (s), 657 (m), 615 (m). EI/MS spectra were obtained on a Kratos Analytical mass spectrometer at 70 eV using electron impact ionization; samples were introduced as solids using a direct inlet probe techniques and were typically heated to 150 °C. FAB mass spectra were taken on a Joel VG 70 SEQ tandem hybrid instrument of EBqQ geometry. Samples were quickly introduced into the matrix (4-nitro-benzyl alcohol) as methylene chloride solutions.

$KOs(N)O_3$ was prepared from OsO_4 by literature methods[15] or purchased from Colonial and used without further purification. KTp was synthesized by literature methods.[63] Triphenylphosphine was purchased from Strem and used as received. The reported syntheses of $[^nBu_4N][Os(N)Ph_4]$ and $[^nBu_4N][Os(N)Ph_2Cl_2]$[20] were modified to use an aerobic, aqueous workup. $B(C_6F_5)_3$ was generously supplied by Professor K. I. Goldberg. All other reagents were purchased from Aldrich and used without further purification. Solvents were degassed and dried according to standard procedures.[64] Chromatography was on silica gel unless otherwise noted.

$TpOs(N)Cl_2$ (1). A 250 mL round-bottom flask was charged with 7.00 g (27.8 mmol) of KTp, 120 mL of dry ethanol, and 32.0 mL of concentrated aqueous HCl. $KOsNO_3$ (2.00 g, 6.87 mmol) was added, resulting in a deep purple-colored solution. The solution was refluxed for 30 min, turning a reddish orange color, and then it was cooled and placed in a freezer overnight. The chilled solution was filtered, and a mixture of white and orange-red solids was collected. The solids were rinsed with ~100 mL of H_2O and ~20 mL of ethanol and air-dried for several hours, yielding 1.50 g of **1** (3.07 mmol, 45% yield) as a red-orange power. To remove the $TpOsCl_3$ impurity, 250 mg of **1** (0.51 mmol) containing 5 mol % $TpOsCl_3$ (as determined by ^1H NMR) was dissolved in CH_2Cl_2, and ferrocene (4.83 mg, 0.026 mmol, 1.05 equiv based on $TpOsCl_3$) was added. After the solution was stirred for 1 h, the solvent was removed, and the resulting solid was purified by chromatography and two recrystallizations, affording red plates suitable for X-ray crystallography. ^1H NMR ($CDCl_3$): 6.03 (t), 7.42 (d), 7.52 (d) (each 1H, pz); 6.55 (t), 7.88 (d), 8.38 (d) (each 2H, pz′). $^{13}C\{^1H\}$ NMR ($CDCl_3$): 106.3, 134.5, 143.9 (pz trans to N), 108.6, 138.1, 146.5 (pz trans to Cl). EI/MS: 489 (M^+), 455 (M^+ − Cl). IR: 2516 (B−H), 1066 (Os≡N). Anal. Calcd (found) for $C_9H_{10}BCl_2N_7Os$: C, 22.14 (22.35); H, 2.06 (2.09); N, 20.09 (19.89).

$TpOs(^{15}N)Cl_2$ was prepared on the same scale from $KOs(^{15}N)O_3$ (from OsO_4 + $^{15}NH_4OH$). IR: 1036 ($\upsilon_{Os\equiv{}^{15}N}$).

TpOs(N)(Ph)Cl (2). A glass bomb was loaded with **3** (35 mg, 0.060 mmol), 5 mL of CH_2Cl_2, and then 1 M HCl in Et_2O (0.435 mL, 0.435 mmol; 7.25 equiv) and then heated at 60 °C for 2 days. Column chromatography using toluene as an eluant yielded 15 mg (0.028 mmol, 47%) of orange powder. ^1H NMR ($CDCl_3$): 5.94, 6.43, 6.53 (each 1H, t, pz), 7.00, 7.47, 7.79, 7.88, 7.92, 8.50 (each 1H, d, pz), 7.15 (1H, t, 7 Hz; para), 7.25 (2H, t, 7 Hz; meta), 7.35 (2H, d, 7 Hz; ortho). $^{13}C\{^1H\}$ NMR: 106.7, 108.5, 109.1, 135.1, 137.9, 138.7, 145.0, 146.4, 148.4 (all pz), 127.3, 128.1, 142.8 (all −Ph, *p*, *m*, *o*, ipso not observed). EI/MS: 531 (M^+), 495 (M^+ − Cl).

$TpOs(N)Ph_2$ (3). Concentrated aqueous HI (1 mL) in air was added to a stirred solution of $[nBu_4N][Os(N)Ph_4]$ (400 mg, 0.530 mmol) in 100 mL of acetone, resulting in a rapid color change from yellow to bright orange. After 5 min, KTp (200 mg, 0.794 mmol) was added, and the solution gradually darkened. This mixture was heated briefly to 60 °C and then allowed to stir for 4 h at room temperature. Chromatography using toluene as an eluant gave **3** (100 mg, 0.175

(62) Alves, A. S.; Moore, D. S.; Andersen, R. A.; Wilkinson, G. *Polyhedron* **1982**, *1*, 83−87.

(63) Trofimenko, S. *J. Am. Chem. Soc.* **1966**, *88*, 1842−1844.

(64) Perrin, D. D.; Armarego, W. L. F. *Purification of Laboratory Chemicals* 3rd ed.; Pergamon Press: New York, 1988.

mmol, 33%) as an orange powder. ^{1}H NMR ($CDCl_3$): 5.99 (t, 1H, t, pz), 6.38 (2H, t, pz′), 6.86, 7.55 (each 1H, d, pz), 7.80, 7.89 (each 2H, d, pz′), 7.02 (2H, t, 7 Hz; para), 7.15 (4H, t, 7 Hz; meta), 7.36 (4H, d, 7 Hz; ortho). ^{13}C{^{1}H} NMR: 105.4, 134.5, 144.8 (pz trans to N), 107.1, 136.8, 146.2 (pz trans to Ph), 125.1 (para), 127.4 (meta), 141.4 (ortho), 155.1 (ipso). EI/MS: 572 (M^+), 495 ($M^+ - Ph$). Anal. Calcd (found) for $C_{21}H_{20}BN_7Os$: C, 44.14 (44.74); H, 3.53 (3.69); N, 17.16 (17.24).

TpOs(NHPh)Cl$_2$ (4). PhMgBr in THF (200 mg in ∼10 mL) was added dropwise over 5 min to a −78 °C solution of **1** (100 mg, 0.204 mmol) in 20 mL of THF, resulting in a darkening of the orange solution. The solution was stirred at −78 °C for 1 h, and then at room temperature for 1 h, and then was exposed to the atmosphere, resulting in a rapid color change from dark orange to deep red. Chromatography using 50:50 CH_2Cl_2/hexanes allowed the isolation of **4** (94 mg, 0.165 mmol, 81%). ^{1}H NMR ($CDCl_3$): −3.50 (d, 7.0 Hz, 2H, *NPh$_o$*), 8.69 (t, 7.0 Hz, 2H, *NPh$_m$*), 0.01 (t, 7.0 Hz, 1H, *NPh$_p$*), 5.50 (br s, 1H, NH), 6.06 (t, 1H, pz), 5.38, 6.19 (each d, 1H, pz), 6.62 (t, 2H, pz′) 6.82, 4.59 (each d, 2H, pz′). IR: 3519 (NH), 2508 (BH). EI/MS: 567 (M^+). Anal. Calcd (found) for $C_{15}H_{16}BCl_2N_7Os$: C, 31.81 (31.87); H, 2.85 (2.98); N, 17.33 (16.87). UV/vis (CH_2Cl_2) [nm (ϵ, M^{-1} cm^{-1})]: 256 (12 300), 339 (8200), 420 (7700), 504 (12 800).

TpOs(NHTol)Cl$_2$ (5). A bomb was charged with toluidine (15.5 mg, 145 μmol), **1** (63.6 mg, 130 μmol), and 5 mL of CH_2Cl_2. The bomb was heated at 70 °C for 1 day and then opened in the atmosphere, and another 15.0 mg (141 μmol) of toluidine was added. The bomb was heated for another 6 days at 70 °C. Column chromatography with CH_2Cl_2 as the eluant yielded 32 mg of red/violet powder **5** (55 μmol, 42%) in addition to ∼20 mg of **1**. ^{1}H NMR ($CDCl_3$): 6.14 (t, 1H, pz), 6.56, 5.78 (each d, 1H, pz), 6.58 (t, 2H, pz′), 6.68, 5.05 (each d, 2H, pz′), 8.02, −2.39 (each d, 2H, 7 Hz, tolyl), 10.26 (s, 3H, CH_3), 7.59 (br s, 1H, NH). EI/MS: 581 (M^+), 545 ($M^+ - Cl$).

TpOs(NHPh)(Ph)Cl (6). A procedure analogous to that for **4** was used, with 2 equiv of PhMgBr. ^{1}H NMR ($CDCl_3$): −2.49 (d, 7.5 Hz, 2H, *NPh$_o$*), 8.57 (t, 7.5 Hz, 2H, *NPh$_m$*), 1.00 (t, 7.5 Hz, 1H, *NPh$_p$*), 2.27 (d, 7.5 Hz, 2H, *OsPh$_o$*), 8.54 (t, 7.5 Hz, 2H, *OsPh$_m$*), 3.93 (t, 7.5 Hz, 1H, *OsPh$_m$*), 11.5 (br, 1H, NH), 6.92, 6.70, 5.88 (t, 1H, pz), 7.62, 6.36, 6.21, 5.63, 4.99, 4.73 (d, 1H, pz). EI/MS: 609 (M^+).

TpOs(NHPh)Ph$_2$ (7). A procedure analogous to that for **4** was used, with 3 equiv of PhMgBr. ^{1}H NMR (CD_2Cl_2): −3.66 (d, 7.5 Hz, 2H, *NPh$_o$*), 8.69 (t, 7.5 Hz, 2H, *NPh$_m$*), −0.69 (t, 7.5 Hz, 1H, *NPh$_m$*), 1.55 (d, 7.5 Hz, 4H, *OsPh$_o$*), 9.17 (t, 7.5 Hz, 4H, *OsPh$_m$*), 3.50 (t, 7.5 Hz, 2H, *OsPh$_m$*), 12.1 (br, 1H, N*H*), 5.84 (t, 1H, pz), 5.62, 4.08 (d, 1H, pz), 6.91 (t, 2H, pz′), 7.61, 5.46 (d, 2H, pz′). IR: 3526 (NH), 2514 (B−H). EI/MS: 650 (M^+).

TpOs(NPh)Ph$_2$MgCl. A screwtop NMR tube was charged with 50 μL of 2 M PhMgCl in THF (0.100 mmol). The solvent was removed in vacuo, and 0.50 mL of C_6D_6 was condensed in. The tube was shaken, and then the solvent was stripped off in vacuo. The tube was brought into the box, where it was charged with 14.0 mg (0.028 mmol, 0.28 equiv) of **1**. The contents were dissolved in 1 mL of C_6D_6, resulting in a dark orange solution of TpOs(NPh)Ph$_2$MgCl as determined by ^{1}H NMR: 2.86 (d, 7.5 Hz, 2H, *NPh$_o$*), 8.21 (t, 7.5 Hz, 2H, *NPh$_m$*), 4.25 (t, 7.5 Hz, 1H, *NPh$_m$*), 5.75 (d, 7.5 Hz, 4H, *OsPh$_o$*), 7.88 (t, 7.5 Hz, 4H, *OsPh$_m$*), 6.02 (t, 7.5 Hz, 2H, *OsPh$_m$*), 5.88 (t, 1H, pz), 6.14, 6.78 (d, 1H, pz), 6.12 (t, 2H, pz′), 6.81, 6.85 (d, 2H, pz′).

TpOs(H$_2$NEt)Cl$_2$ (8). Et_2Zn (0.200 mmol in 20 mL of THF) was added dropwise over 5 min to a −78 °C solution of **1** (0.100 mg, 0.204 mmol) in 35 mL of THF. The solution immediately turned dark purple. After being stirred for 3 h at −78 °C and 5 h at room temperature, the solution was exposed to air, affording a dark brown solution. Purification by silica gel chromatography and recrystallization in air from acetone/heptane gave NMR-silent **8** (27.5 mg, 0.053 mmol, 26%) as red plates. IR (KBr): 3241, 2967, 2505 (B−H), 1704, 1500, 1408, 1308, 1213, 1115, 1047, 838, 782, 711, 620. DIP/MS: 520 (M^+), 475 ($M^+ - H_2NEt$). Anal. Calcd (found) for $C_{11}H_{17}BCl_2N_7Os$: C, 25.45 (25.63); H, 3.30 (3.47); N, 18.88 (19.01).

TpOs(H$_2$NMe)Cl$_2$ (9). Following the procedure for **8**, MeMgCl (0.200 mmol in 20 mL of THF) was added to **1** (0.100 mg, 0.204 mmol in 35 mL of THF) and stirred at −78 °C for 1 h, and then at 20 °C for 2 h. Exposure to air afforded a blue solution. Purification by silica gel chromatography and recrystallization in air from CH_2Cl_2/heptane gave dark orange **9** (35.9 mg, 0.071 mmol, 35% yield) as dark orange plates. IR (KBr): 3566, 3244, 2954, 2497 (B−H), 1713, 1592, 1499, 1408, 1306, 1210, 1118, 1074, 1049, 763, 708, 655, 618. DIP/MS: 506 (M^+), 475 ($M^+ - H_2NEt$). Anal. Calcd (found) for $C_{10}H_{15}BCl_2N_7Os$: C, 23.78 (24.11); H, 2.99 (3.22); N, 19.41 (19.07).

TpOs(NHEt)Cl$_2$ (10). A solution of **16** (generated in situ, see below) was exposed to air for approximately 10 min, and 2 μL of H_2O was added. The solution slowly turned a pale yellow. ^{1}H NMR (CD_2Cl_2): 6.27 (t, 1H, pz), 6.98, 6.55 (d, 1H, pz), 6.50 (t, 2H, pz′), 6.27, 7.17 (d, 2H, pz′), 19.24 (q, 6.7 Hz, 2H, NCH_2CH_3), 1.24 (t, 6.7 Hz, 3H, NCH_2CH_3), 3.4 (br, N*H* + H_2O). FAB/MS: 519 (st, M^+), 483 (v st, $M^+ - Cl$). Attempts to work up **10** by column chromatography following the procedures for **4**−**7** yielded only ^{1}H NMR-silent yellow materials.

TpOs[N(Ph)(BPh$_2$)]Cl$_2$ (11). A flask charged with 180 mg of **1** (0.368 mmol), 108 mg of BPh_3 (0.446 mmol, 1.21 equiv), and 10 mL of C_6H_6 was stirred for 5 min. Filtering, layering the filtrate with 60 mL of hexanes, and it allowing to stand overnight yielded dark orange **11** (138 mg, 52%). ^{1}H NMR ($CDCl_3$): 6.29 (t, 1H, pz), 6.94, 7.47 (d, 1H, pz), 6.12 (t, 2H, pz′), 6.05, 7.00 (d, 2H, pz′), 4.50 (d, 7 Hz, 2H, *NPh$_o$*), 7.26 (t, 7 Hz, 2H, *NPh$_m$*), 6.90 (t, 7 Hz, 1H, *NPh$_p$*), 7.63 (d, 7 Hz, 4H, *BPh$_{2ortho}$*), 7.32 (t, 7 Hz, 4H, *BPh$_{2meta}$*), 7.43 (t, 7 Hz, 2H, *BPh$_{2para}$*). Anal. Calcd (found) for $OsC_{27}H_{25}N_7B_2Cl_2$: C, 44.40 (44.03); H, 3.45 (3.42); N, 13.43 (13.42).

TpOs[N(Ph)(BPhOBPh$_2$)]Cl$_2$ (12). Compound **12** was prepared as for **11** except with stirring overnight. Isolated yield: 34%. ^{1}H NMR ($CDCl_3$): 5.96 (1H, t, pz), 5.73, 4.72 (each 1H, d, pz), 6.69 (2H, t, pz′), 6.96, 4.12 (each 2H, d, pz′); Ph, 9.20 (2H, t), 7.70 (4H, t), 7.47 (1H, t), 4.10 (2H, t), 1.91 (1H, t), 1.27 overlapping (3H, d), 0.89 (2H, t), −4.10 (4H, t). Repeated submittals of the same sample gave substantially different elemental analyses, indicating analytical difficulties.

B(Tol)$_3$ was prepared by addition of LiTol in pentane (from $PhCH_2I$, 2.18 g, 10 mmol + ^{n}BuLi, 6.25 mL/1.6 M in hexanes, 10 mmol) to a pentane solution of BBr_3 (0.32 mL, 3.4 mmol). Filtration and removal of the volatiles gave 0.75 g (2.6 mmol, 76%) of white B(Tol)$_3$. ^{1}H NMR ($CDCl_3$): 7.71, 7.25 (d, 7 Hz, 2H each), 2.43 (s, 3H). EI/MS: 284 (M^+), 193 ($M - Tol^+$).

BPh(Tol)$_2$ was prepared similarly from $PhCH_2I$ (3.26 g, 15 mmol), ^{n}BuLi (9.4 mL/1.6 M in hexanes, 15 mmol), and $PhBCl_2$ (0.97 mL, 7.5 mmol). The white product (0.50 g, 1.85 mmol, 25%) was sublimed and recrystallized from pentane. ^{1}H NMR ($CDCl_3$): 7.54, 7.27 (d, 2 Hz, 4H, Tol), 7.60 (d, 2H), 7.52 (t, 1H), 7.43 (t, 2H, each 8 Hz, Ph *o*, *p*, *m*).

TpOs(N(C$_6$F$_5$)[B(C$_6$F$_5$)$_2$])Cl$_2$ (13). A solution of **1** (78 mg, 160 μmol), $B(C_6F_5)_3$ (78 mg, 152 μmol), and 40 mL of benzene was stirred for 10 min. The solvent was removed, and the solids were extracted with 100 mL of pentane. Removal of the pentane yielded **13** (80 mg, 80 μmol, 53% yield) as a reddish orange powder. ^{1}H NMR ($CDCl_3$): 0.80 (t, 1H, pz), −3.28 (d, 1H, pz), −18.62 (br, 1H, pz), 5.32 (t, 2H, pz′), 8.66 (d, 2H, pz′), −23.31 (br, 2H, pz′). ^{19}F NMR: 3.9 (br s, 2F), −19.5 (br s, 2F), −39.4 (br s, 2F), −76.8 (br s, 1F), −84.0 (br s, 4F), −85.9 (br s, 4F).

TpOs[NH(C$_6$F$_5$)]Cl$_2$ (14). A methylene chloride solution of **13** was exposed to air, resulting in an immediate color change from dark orange to vivid purple. Purification of the solution by short column chromatography yielded **14** in 90% yield. ^{1}H NMR ($CDCl_3$): 4.99 (t, 1H, pz), 1.46, 1.34 (d, 1H, pz), 6.61 (t, 2H, pz′), 7.76, −1.19 (d, 2H, pz′). ^{19}F NMR ($CDCl_3$): 0.2 (d, 6 Hz, 2F, *ortho*), −120.4 (t, 6 Hz, 2F, *meta*), 36.9 (t, 6 Hz, 1F, *para*). FAB/MS: 658 (strong, M^+), 623 (strong, $M^+ - Cl$), 475 (very strong, $M^+ - NH(C_6F_5)$).

TpOs[N(Et)BEt$_2$]Cl$_2$ (15). A screwtop NMR tube was loaded with **1** (4.3 mg, 8.8 μmol) and 0.5 mL of methylene chloride. Addition of BEt_3 (10 μL, 1 M in THF, 10 μmol) resulted in an immediate color change to vibrant yellow. The solvent was removed in vacuo, and 0.5 mL of $CDCl_3$ was condensed in. ^{1}H NMR ($CDCl_3$): 6.33 (t, 1H, pz), 7.50, 7.26 (d, 1H, pz), 6.34 (t, 2H, pz′), 7.14, 7.05 (d, 2H, pz′), 0.91 (t, 7.4 Hz, 3H, NCH_2CH_3), 7.100 (obscured q, 2H, NCH_2CH_3), 1.29 (br s, 10H, BCH_2CH_3). FAB/MS: 587 (w, M^+), 572 (vw, $M^+ - Me$), 558 (w, $M^+ - Et$), 552 (w, $M^+ - Cl$), 537 ($M^+ - MeCl$), 519 (st, $M^+ - BEt_2$), 483 (v st, $M^+ - BEt_2Cl$).

TpOs{N(Et)[BEt(OMe)]}Cl_2 (16). A screwtop NMR tube was loaded with **1** (8.0 mg, 16.4 μmol) and 0.5 mL of CD_2Cl_2. $Et_2B(OMe)$ (2.5 μL, 19 μmol) was added, and the color of the solution changed from orange to dark yellow over 40 min. ^{1}H NMR (CD_2Cl_2): 6.19 (t, 1H, pz), 6.21, 6.68 (d, 1H, pz), 6.56 (t, 2H, pz′), 5.99, 7.32 (d, 2H, pz′), 4.38 (s, 3H, O*Me*), 1.52 (t, 7.3 Hz, 3H, BCH_2CH_3), 1.44 (d, 8.3 Hz, 2H, NCH_2CH_3), 0.67 (t, 8.3 Hz, 3H, NCH_2CH_3), 15.9 (br s, 2H, BCH_2CH_3). $^{13}C\{^1H\}$ NMR (CD_2Cl_2): 149.7, 136.9, 102.8 (pz, 1C), 150.0, 135.0, 102.8 (pz′, 2C).

TpOs[NB(C_6F_5)$_3$]Ph_2 (17). An NMR tube was charged with **3** (12.4 mg, 22 μmol), B(C_6F_5)$_3$ (12.3 mg, 24 μmol), and then CD_2Cl_2 (0.5 mL). Upon thawing, a green solution was observed, whose ^{1}H NMR did not change on heating for 8 h at 80 °C. Removal of the CD_2Cl_2 and recrystallization from benzene gave air-sensitive green crystals suitable for X-ray analysis. ^{1}H NMR (CD_2Cl_2): 5.89 (t, 1H, pz), 6.33, ~7.00 (d, 1H, pz), 6.39 (t, 2H, pz′), 7.71, 8.00 (d, 2H, pz′), 6.98 (d, 7 Hz, 4H, *OsPh$_o$*), 7.18 (t, 7 Hz, 4H, *OsPh$_m$*), 7.05 (t, 7 Hz, 2H, *OsPh$_m$*). ^{19}F NMR (CD_2Cl_2): −54.4 (d, 18 Hz, 6F, *ortho*), −81.6 (t, 19 Hz, 3F, *para*), −88.3 (t, 18 Hz, 6F, *meta*).

Crystal Structures of 3, 4, and 8. Crystals were grown by slow evaporation of hexane (**3**), hexane/ethyl acetate (**4**), or acetone/heptane solutions (**8**). Crystals were mounted on a glass fiber with epoxy (**3**, **4**) or in a glass capillary in oil (**8**). Data were collected on a Nonius KappaCCD diffractometer, by rotation about the ϕ axis in 1° increments over 360°. The exposure times per frame and the crystal−detector distances were 60 s and 27 mm for **3**, 30 s and 30 mm for **4**, and 30 s and 27 mm for **8**. The merging *R* factors of 0.052 (**3**), 0.037 (**4**), and 0.056 (**4**) indicated the data were all of good quality. Solutions by direct methods produced a complete phasing model for **3** and **8**, and an almost complete phasing model for **4**, with the rest located by difference Fourier synthesis. In **3** and **4** there are two independent molecules in the asymmetric unit. **8** crystallizes with one molecule of acetone; both the Os complex and the solvent reside on a mirror plane. All heavy atoms were refined anisotropically by full matrix least-squares. For **3**, hydrogen atoms H1A, 2A, 3, 6, 7, 8, 9, 11, 12, 13, 15, 19, 20, 22, 23, 24, 25, 28, 32, 33,35, 36, 39, 41, and 42 were located in the difference maps; the remaining ones were placed in calculated positions. For **4** and **8**, all hydrogen atoms were placed in calculated positions, except for the boron hydrogen in **8** (H1B). Hydrogens were given isotropic parameters of 1.1U_{eq} of their parent atom (**3**) or fixed isotropic parameters of 0.05 (**4**) and refined with a riding model. The min/max residual electron densities were located near the Os atom and were not of chemical significance. Empirical absorption corrections were applied before structure solution.

Crystal Structures of 11 and 12. Crystals of **11** and **12**, obtained on slow evaporation from $CH_2Cl_2/Me_3SiOSiMe_3$ solutions, were immersed in oil and mounted under a stream of N_2. Data were collected on an Enraf-Nonius CAD4 Diffractometer. Semiempirical absorption corrections used ψ-scans. Full-matrix least-squares refinement used SHELXL-97.[65] All heavy atoms were located in the Patterson map and refined anisotropically; hydrogen atoms were placed in calculated positions and refined using a riding model. Crystals of **13** were grown by slow evaporation of a benzene solution; the structure is described in the Supporting Information.

Crystal Structure of TpOs[NB(C_6F_5)$_3$]Ph_2 (17). A green, prismatic crystal of **17** was immersed in oil and mounted on a glass capillary with epoxy under a stream of nitrogen. Data were collected on a Nonius KappaCCD with two sets of 10 s exposures using a κ offset of 100 between the two sets. An empirical correction for absorption anisotropy was applied before structure solution.[66] Solution by Patterson methods produced a complete phasing model consistent with the proposed structure.[67] Two benzene molecules of crystallization were located by difference Fourier synthesis.[68] All hydrogen atoms were placed with idealized geometry and were refined isotropically with a riding model with U_{iso} values fixed at 1.1U_{eq} of their parent atom. All non-hydrogen atoms were refined anisotropically.

Computational Details. All computations were performed using the GAUSSIAN-94 package.[69] The geometries of all molecules were optimized using idealized molecular symmetries at the RHF/LANL2MB level of theory. Complexes **4** and **5** were also optimized at the Xα/LANL2DZ level of theory. Single-point calculations were then performed on all molecules using Xα/LANL2DZ.

Acknowledgment. We gratefully acknowledge the NSF for support to J.M.M. and for support of an upgrade of our 500 MHz NMR spectrometers (Grant No. 9710008).

Supporting Information Available: Crystallographic data for **1**, **3**, **5**, **8**, **9**, **11**, **12**, **13**, and **17** (for **4**, see ref 10a) (PDF). This material is available free of charge via the Internet at http://pubs.acs.org.

JA0028424

(65) Sheldrick, G. M. SHELXL93. In *Crystallographic Computing 6*; Flack, P., Parkanyi, P., Simon, K., Eds.; IUCr/Oxford University Press: Oxford, U.K., 1993.

(66) Blessing, R. H. *Acta Crystallogr.* **1995**, *A51*, 33.

(67) Beurskens, P. T.; Admirall, G.; Beurskens, G.; Bosman, W. P.; Garcia-Granda, S.; Gould, R. O.; Smits, J. M. M.; Smykalla, C. *DIRDIF*, University of Nijmegen, Nijmegen, The Netherlands.

(68) Sheldrick, G. M. SHELXL97, Program for the Refinement of Crystal Structures, University of Gottingen, Gottingen, Germany.

(69) Frisch, M. J.; Trucks, G. W.; Schlegel, H. B.; Gill, P. M. W.; Johnson, B. G.; Robb, M. A.; Cheeseman, J. R.; Keith, T.; Petersson, G. A.; Montgomery, J. A.; Raghavachari, K.; Al-Laham, M. A.; Zakrzewski, V. G.; Ortiz, J. V.; Foresman, J. B.; Peng, C. Y.; Ayala, P. Y.; Chen, W.; Wong, M. W.; Andres, J. L.; Replogle, E. S.; Gomperts, R.; Martin, R. L.; Fox, D. J.; Binkley, J. S.; Defrees, D. J.; Baker, J.; Stewart, J. P.; Head-Gordon, M.; Gonzalez, C.; Pople, J. A., *Gaussian 94*, Revision B.3; Gaussian, Inc.: Pittsburgh, PA, 1995.